Multi-pollutants emissions from the burning of major agricultural residues in China and the related health-economic effect assessment

Chunlin Li[1], Yunjie Hu[1], Fei Zhang[1], Jianmin Chen[1,2], Zhen Ma[1], Xingnan Ye[1], Xin Yang[1,2], Lin Wang[1,2], Xingfu Tang[1], Renhe Zhang[2], Mu Mu[2], Guihua Wang[2], Haidong Kan[3], Xinming Wang[4], Abdelwahid Mellouki[5]

[1]Shanghai Key Laboratory of Atmospheric Particle Pollution and Prevention (LAP[3]), Department of Environmental Science & Engineering, Fudan University, Handan Road 220, Shanghai 200433, China

[2]Institute of Atmospheric Sciences, Fudan University, Handan Road 220, Shanghai 200433, China

[3]Public Health School, Fudan University, Dongan Road 120, Shanghai 200032, China

[4]State Key Lab of Organ Geochemistry, Guangzhou Institute of Geochemistry, Chinese Academy of Sciences, Kehuajie Road 511, Guangzhou 510640, China

[5]Institut de Combustion, Aérothermique, Réactivité et Environnement, CNRS, 45071 Orléans cedex 02, France

Correspondence to: J. M. Chen (jmchen@fudan.edu.cn)

Abstract. Multi-pollutants in smoke particulate matter (SPM) were identified and quantified for biomass burning of five major agricultural residues such as wheat, rice, corn, cotton, and soybean straws in China by aerosol chamber system combining with various measurement techniques. The primary emission factors (EFs) for $PM_{1.0}$ and $PM_{2.5}$ are 3.04-12.64 and 3.25-15.16 g kg^{-1}. Organic carbon (OC), elemental carbon (EC), water-soluble inorganics (WSI), water-soluble organic acids (WSOA), water-soluble amine salts (WSA), trace mineral elements (THM), polycyclic aromatic hydrocarbons (PAHs), and phenols in smoke $PM_{1.0}/PM_{2.5}$ are 1.34-6.04/1.54-7.42, 0.58-2.08/0.61-2.18, 0.51-3.52/0.52-3.81, 0.13-0.64/0.14-0.77, (4.39-85.72/4.51-104.79)×10^{-3}, (11.8-51.1/14.0-131.6)×10^{-3}, (1.1-4.0/1.8-8.3)×10^{-3}, and (7.7-23.5/9.7-41.5)×10^{-3} g kg^{-1}, respectively. BC mainly exist in $PM_{1.0}$, heavy metal-bearing particles favor to reside in the range of smoke $PM_{1.0-2.5}$, which are also

confirmed by individual particle analysis.

With respect to five scenarios of burning activities, the average emissions and overall propagation of uncertainties at 95% confidence interval (CI) of SPM from agricultural open burning in China in 2012 were estimated for $PM_{2.5}$, $PM_{1.0}$, OC, EC, WSI, WSOA, WSA, THM, PAHs, and phenols to be 1005.7 (-24.6% , 33.7%), 901.4 (-24.4%, 33.5%), 432.4 (-24.2%, 33.5%), 134.2 (-24.8%, 34.0%), 249.8 (-25.4%, 34.9%), 25.1 (-33.3%, 41.4%), 5.8 (-30.1%, 38.5%), 8.7 (-26.6%, 35.6%), 0.5 (-26.0%, 34.9%), and 2.7 (-26.1%, 35.1%) Gg, respectively. The emissions were further temporal-spatially characterized using geographic information system (GIS) at different regions in summer and autumn post-harvest periods. It was found less than 25% of the total emissions were released during summer harvest that was mainly contributed by the North Plain and the Central of China, especially Henan, Shandong, and Anhui, leading the top three provinces of smoke particle emissions.

Flux concentrations of primarily emitted smoke $PM_{2.5}$ that were calculated using box-model method based on five versions of emission inventories all exceed the carcinogenic risk permissible exposure limits (PEL). The health impacts and health-related economic losses from the smoke $PM_{2.5}$ short-term exposure were assessed. The results show that China suffered from 7836 (95% CI: 3232, 12362) premature mortality and 7267237 (95% CI: 2961487, 1130784) chronic bronchitis in 2012, which led to 8822.4 (95% CI: 3574.4, 13034.2) million US$, or 0.1% of the total GDP losses. We suggest that percentage of open burnt crop straws at post-harvest period should be cut down by over 97% to ensure risk aversion from carcinogenicity, especially the North Plain and the Northeast, where the emissions should decease at least by 94% to meet the PEL. Under such emission control, over 92% of the mortality and morbidity attributed to agricultural fire smoke $PM_{2.5}$ can be avoided in China.

1 Introduction

Biomass burning (BB) is a significant source of particulate- and gaseous- pollutants (Andreae and Merlet, 2001; Clarke et al., 2007; Ram et al., 2011; Saikawa et al.,

2009a; Tian et al., 2008). It was estimated that open burning of biomass contributed approximately 40% of the globally averaged annual submicron black carbon (BC) aerosol emissions and 65% of primary OC emissions (Bond et al., 2013). China is the major contributor that bears over 24% of global emissions of carbonaceous aerosols, especially from agricultural field burning, about 0.04~0.5 Tg EC and 0.4~2.1 Tg OC are released annually (Bond, 2004; Cao et al., 2006; Qin and Xie, 2012; Saikawa et al., 2009), resulting in great radiative forcing, air quality deterioration, visibility reduction, premature mortality, and economic loss regionally and globally (Bølling et al., 2009; Bond et al., 2013; Huang et al., 2014; Janssen et al., 2011; Rosenfeld, 2006; Saikawa et al., 2009; Shindell et al., 2012).

BB also represents one of the most uncertainties in the emission, climate effect, and public health assessments, which finally relies on the uncertainties in detailed chemical emissions or related properties and burning activities like strength or percentage of biomass fuel burned (Tian et al., 2008; Andreae and Merlet, 2001; Levin et al., 2010). For example, studies have focused on OC and EC emissions due to their specific optical properties (Bond et al., 2013; Cao et al., 2006; Qin and Xie, 2012; Ram et al., 2011). OC like sulfate and nitrate can cool the atmosphere by increasing the Earth's reflectivity, however, smoke OC on the other hand has been treated as brown carbon to exhibit pronounced light absorption character (Chen et al., 2015; Ackerman, 2000; Chakrabarty et al., 2010; Christopher et al., 2000). The coated or internal mixed sulfate or nitrate can act as lens to enhance the light absorption activity of BC (Zhang et al., 2008b), probably also the activity of brown carbon (Chen et al., 2015). However, primary emissions for OC, EC, and alkali components are confused and have a wide range (Sen et al., 2014; Cao et al., 2006; Hayashi et al., 2014), and some study still took OC with negative forcing activity (Saikawa et al., 2009; Shindell et al., 2012). Besides, smoke EC is consisting of soot and char, and soot-EC has a higher light-absorption potential compared to char-EC (Arora and Jain, 2015; Reid et al., 2005a). Division and quantification of char- and soot-EC emissions for biomass burning are understudied (Arora and Jain, 2015; Han et al., 2007, 2009). Moreover, other components like organic acids, amines, phenols, and mineral elements that

enable CCN activity or endow health hazard of smoke aerosol are also deficient, variable, or outdated, which may hinder our overall understanding of biomass burning contributions and also atmospheric process of smoke particles (Li et al., 2015; Akagi et al., 2011; Chan et al., 2005; Dhammapala et al., 2007a; Ge et al., 2011; Reid et al., 2005a, b).

Studies using carbon mass-balance (CMB) and pollutant concentration-chamber volume quantification are the two common methods to derive the emission factors for biomass burning aerosols (Akagi et al., 2011; Li et al., 2007; Zhang et al., 2008a). Carbonaceous and inorganics components of smoke particles not only vary with biomass issues (fuel types, water content, or burning strength), but also relate to burning condition and environment (flaming or smoldering, field burning or laboratory simulation), extent of aging, sampling methods, and measurement technologies (Grieshop et al., 2009; Hayashi et al., 2014; Reid et al., 2005b). Comparing to field observations that are closer to the actual burning (Li et al., 2007; Akagi et al., 2011; Rose et al., 2011; Saffari et al., 2013), laboratory studies have a definite advantage over field burning research in emission analysis (Jayarathne et al., 2014; Sun et al., 2016; Zhang et al., 2008a). For example, the environment, amount of fuel, and burning conditions can be precisely controlled, the contamination from ambient atmosphere to the emissions can be excluded, and chemical compositions at different aging extent can be quantified using aerosol chamber system (Li et al., 2015, 2016; Aurell et al., 2015; Dhammapala et al., 2007b).

The activity rates of biomass burning (burning rate of biomass fuels) are also response to the great uncertainties in the emission estimates (Sun et al., 2016; Zhang et al., 2008a). Seldom study ever focused on the burning rates, and the limited data were treated as simplex constant or dynamic values in many studies of emission estimation in a certain year or for annual variations with a long time scales, thus, significant difference among the results were founded (Qin and Xie, 2011, 2012; Zhang et al., 2011; Zhao et al., 2012). For instance, Cao et al. (2006, 2011) estimated primary smoke carbonaceous materials emissions for 2000 and 2007 in China with same field burning rates, the results were almost the same for the two year with 103-104 Gg yr^{-1}

BC and 425.9-433.3 Gg yr^{-1} OC emitted. He et al. (2011b) found the declining trends in biomass burning emissions in the Pearl River Delta for the period 2003-2007 based on constant activity data of burning rates. Lu et al. (2011) developed primary carbonaceous aerosol emissions in China for 1996-2010 with time-dependent activity rates extrapolated from 2008 to 2010 based on national fast-track statistic, rapid increase of OC and EC emissions were reported, and OC increased from 1.5 to 2.3 Tg yr^{-1}, BC increased from 418 to 619 Gg yr^{-1}. Qin and Xie (2012) estimated BC emission from crop straw open burning for 1980-2009 with variable burning rates based on peasants' income development, the increasing trend in BC emission was also confirmed, and BC emission increased from 4.3 to 116.6 Gg yr^{-1}.

As most anthropogenic pollutants are concentrated in submicron particulate matters ($PM_{1.0}$) (Ripoll et al., 2015), more pronounced relationship of ambient $PM_{1.0}$ to haze formation and adverse health effect has been reported (Huang et al., 2003; Roemer et al., 2001; Shi et al., 2014). Nevertheless, associated chemical characterization of $PM_{1.0}$ is still undefined (Li et al., 2015; Safai et al., 2013; Cheng et al., 2006). The study of source-specific $PM_{1.0}$ chemical compositions and emissions are necessary to replenish database for contribution assessment and model application in atmospheric chemistry, climate changes, and public health evaluation.

The emission inventories and forecasting in the emissions of atmospheric pollutants have been widely studied, and the incurred mortality, climatic effect, and economic loss have also been estimated (Ostro and Chestnut, 1998; Saikawa et al., 2009; Shindell et al., 2012), based on which the emission control policies were proposed. Shindell et al. (2012) considered ~400 control measures in tropospheric BC and O_3 emissions for the benefit of global or regional human health and food security, and 14 optimal measures targeting CH_4 and BC emissions were identified. Saikawa et al. (2009) compared different scenarios of OC, EC, and sulfate emissions in China in 2030, concluding that maximum feasible reduction may avoid over 480000 premature deaths in China and decrease the radiative force from -97 to -15 mW m^{-2} globally. Wang et al. (2008a) reported field burning restriction may save about 5 billion dollars losses from biological resource and air pollution. However, the generalized strategies

in emission reduction were inadequate and lack actual practicality (Streets, 2007; Lin et al., 2010).

In this study, burning experiments with five major agricultural straws were conducted using a combustion stove in combination with an aerosol chamber system. Accurate compositions and emission factors for SPM in $PM_{1.0}$ and $PM_{2.5}$ were characterized and established. Afterwards, up-to-date emissions for agricultural open burning aerosol in 2012 were developed, health and health-related economic impacts from smoke $PM_{2.5}$ exposure were also assessed. Finally, emission reduction strategy that was implemented in field burning rate control for the carcinogenic risk concern was proposed, which should help establish the policy and provide an idea for the emission control.

2 Methodology

An overview of the research procedures including emission factors acquirement and emission inventory calculation is shown in Fig. 1. Tabulation of emission factors is self-established in our laboratory using a combustion stove to simulate open burning and an aerosol chamber to quantify the emissions. Then, we use a bottom-up approach to calculate the emission inventory of agricultural field burning over China mainland based on crop production data in 2012. Emissions for each species are estimated as:

$$E_{k,j} = \sum_i A_{k,i} \times EF_{i,j} \quad (1)$$

where E_j is emission, $A_{k,i}$ is effective biofuel consumption, and $EF_{i,j}$ is emission factor. k, i, and j indicates region, agricultural residue type, and particulate chemical species.

State-of-the art chemical transport and box models were commonly applied to reproduce or simulate the ambient aerosol concentrations (Ram et al., 2011; Reddy and Venkataraman, 2000; Saikawa et al., 2009). In this study, spatio-temporal dynamic box model is used to calculate the emission flux concentration. Regional crop straws are premised to be combusted proportionally only in the fire occurrence days. Dismissing interaction of emitted pollutants in space and time, pollutants will distribute uniformly in a space covering an area of specific region with mixing height

of 0.5 km (atmospheric boundary layer). The flux concentration of agricultural burning smoke can be calculated by Eq. (2):

$$C_{k,j} = \frac{E_{k,j}}{S_k \times h \times T_k} \quad (2)$$

in Eq. (2), $C_{k,j}$ is flux concentration of smoke aerosol, S_k is regional area, h is boundary layer height, T_k is agricultural field fire duration time.

2.1 Aerosol chamber work and emission factors

2.1.1 Crop straws

Five kinds of representative crop residues were used for the burning experiments, i.e., wheat, rice, corn, cotton, and soybean straws. The straws were collected based on regional features of agricultural planting, winter wheat straws were collected from Anhui province, late rice straws from Shanghai, corn straws from Henan province, cotton and soybean residues from Xinjiang. All straws were stored under dark, airy, and cooling condition. Prior to the burning experiment, the dirt and weeds were removed, then straws were dehydrated (at 100 ^{o}C for 24 h) to minimize effect of the water content on the burning and pollutant emissions, as study found pollutants emissions and combustion efficiencies (CE) are response to water content, increased moisture content enhances the emissions but also alter the chemical compositions of smoke aerosols (Reid et al., 2005b; Aurell et al., 2015; Hayashi et al., 2014). Although straws in the field are not well dried and moisture contents vary with weather, ventilation, and storing times, for the convenience of practical application and comparison of burnings and emissions, water contents of the straws were controlled within 2 wt.%, which has been applied in many studies (Hayashi et al., 2014; Huo et al., 2016; Li et al., 2015; Oanh et al., 2011; Zhang et al., 2008a, 2011). The dry straws were then cut to a length of approximately 10 cm and weighted 10.0 g per serving.

2.1.2 Burning experiments

The experiments were conducted using an aerosol chamber system (Fig. S1 in

supplement information, SI), which was loaded in a temperature-controlled room (18-22 ^{o}C, 40%-60% RH). A stainless combustion stove was self-deigned to simulate typical field burning of crop straws by automatic ignition with LPG (Liquid petroleum gas) in particular, albeit on a small scale (ignition time less than 0.1 s). 10.0 g conditioned residues were sealed in the 0.227 m^3 combustion stove in advance, once ignited, the force-ventilation and HEPA filtrated particle-free air were supplied (300 L min^{-1}). The emissions were immediately injected into a clean, evacuated aerosol chamber. The burning last about 1 min and over 1 m^3 particle-free air flushed the stove to ensure all the emissions were transferred into the chamber.

The chamber was custom-built to quantify the emissions and characterize the physiochemical properties of smoke aerosols, detailed description of the chamber can be found elsewhere (Zhang et al., 2008a, 2011; Li et al., 2015, 2016). Briefly, the chamber has a volume of 4.5 m^3 with 0.3 mm Teflon coating on the inner side, a magnetic fan fixed on the bottom to stir the aerosol uniformly, and a hygroclip monitor (Rotronic, Model IM-4) equipped inside the chamber to measure the temperature and relative humidity of the aerosol. Before experiment, the chamber was flushed with particle-free air for 6 h, oxidized by high concentration ozone (~3 ppm) for 12 h, then flushed and vacuumized, filled with pure dry air to 80 KPa for use. The emissions from straw burning were aspirated into the chamber till room pressure, afterwards, size measurement and sampling of smoke aerosols were conducted from the chamber. For each type of straw, four burning experiments were conducted. The unburned residues were weighted and deducted from 10.0 g after each test.

Modified combustion efficiency (MCE) for each burning was monitored with CO and CO_2 measuring to determine the burning phase and to ensure the repeatability. MCE is defined as $\Delta CO_2/(\Delta CO_2+\Delta CO)$, where ΔCO_2 and ΔCO are the excess molar mixing ratios of CO_2 and CO (Reid et al., 2005b). A gas-chromatograph (GC, model 930, Shanghai, Hai Xin Gas Chromatograph Co., LTD) equipped with a flame ionization detector, an Ni-H convertor, and a stainless steel column (2 m long) packed with 15% DNP was used to measure CO and CO_2 concentrations in the chamber. And MCE were 0.89-0.96 for all the experiments (see in SI, Table S1), indicating flaming

combustion dominated, which were comparable to that in the field burning (Li et al., 2003; Li et al., 2007).

2.1.3 Size and morphology of smoke aerosol

Size distribution (10 nm-10 μm) of smoke particles was measured using a Wide-range Particle Spectrometer (WPS, Model 1000XP, TSI, USA), which has been described by Li et al (2015). Briefly, WPS integrates the function of scan mobility particle sizer (SMPS) and laser particle sizer (LPS), 0.3 L min^{-1} flow is introduced to SMPS part to classify mobility size from 10 nm to 500 nm in 48 bins, and 0.7 L min^{-1} flow is introduced to LPS part to measure aerodynamic diameter from 350 nm to 10 μm in 18 bins. Particle density, refractive index, and scanning time were set as 1.0 g cm^{-3}, 1.45, and 3 min $loop^{-1}$, respectively, and charge correction mode was on for the measurement. A diffusion dryer tube (45 cm in length) filled with descant-silica gel was set prior to the inlet of WPS. Before experiment, WPS was calibrated with certified polystyrene latex spheres (PSL, 40, 80, and 220 nm, Duke Scientific).

SPM from the 5 types crop straws burning were sampled onto copper grids coated with carbon film (carbon type-B, 300-mesh copper, Tianld Co., China) using a single-stage cascade impactor with a 0.5 mm diameter jet nozzle at a flow rate of 1.0 L min^{-1}. The sampler has a collection efficiency of 100% at 0.5 μm aerodynamic diameter. More information about the cascade impactor can be found elsewhere (Fu et al., 2012; Hu et al., 2015). Then, a JEOL-2010F field emission high-resolution transmission electron microscope (FE-HRTEM) coupled with an oxford energy-dispersive X-ray spectrum (EDX) was applied to investigate the morphology, composition, and mixing state of individual particles.

2.1.4 Chemical sampling and analysis

$PM_{1.0}$ and $PM_{2.5}$ samples for each burning were collected onto pretreated quartz filter of 90 mm in diameter (Tissuquartz, Pall Corp., USA) from the chamber using a high-volume Particle Sampler (HY-100, Qingdao Hengyuan S.T. Development Co.,

Ltd) operating at 100 L min^{-1}. Each filter sampling duration time is 5 min, and total 44 samples (including 4 blank samples) were gathered. The quartz microfiber filters were prebaked for 8 h at 450 ^{o}C to eliminate contamination. Before and after the sampling, the filters were weighted using a balance (Sartorius BP211D) with an accuracy of 10 μg, and the filters were balanced in an electronic desiccator (40 % RH, 22 ^{o}C) for 24 h before usage. After weighting, the loaded filters were stored at -20 ^{o}C in a refrigerator for further analysis.

Water soluble species including general inorganic ions (ions: F^-, Cl^-, NO_2^-, NO_3^-, SO_4^{2-}, Na^+, NH_4^+, K^+, Ca^{2+}, Mg^{2+}), organic acids (CH_3COOH, HCOOH, $C_2H_2O_4$, CH_3SO_3H), and seven protonated amines ($MeOH^+$, $TeOH^+$, $MMAH^+$, $DMAH^+$, $TMAH^+$, $MEAH^+$, and $DEAH^+$ for short, corresponding to monoethanolaminium, triethanolaminium, monomethylaminium, dimethylaminium, triethylaminium, monoethylaminium, and diethylaminium) were measured from 1/4 of each filter with ion chromatography (IC, Model 850 Professional IC, Metrohm, USA) consists of a separation column (Metrosep A Supp 7 250/4.0 for anion and organic acids, Metrosep C-4 150/4.0 for cation, and Metrosep C4-250/4.0 for water soluble aminiums). Sampled filters were ultrasonically extracted with 15.0 mL deionized water (Mili-Q water, 18.2 MΩ·cm), extracted solutions were filtrated using 0.2 μm filters before injected into IC for measurement. Detection limits (DLs) for the ions and aminiums were within 0.5~3.5 ng mL^{-1}, the correlation coefficients for all calibration curves were better than 0.99, and recovery rates for aminiums were in the range of 93%~106% (see in SI, Table S2). Details for the aminium measurements can be found in the work of Tao et al. (2016).

1/4 of each filter was acid dissolved to measure the selected elements (As, Pb, Cr, Cd, Ni, V, Zn, Al), of which As, Zn, Pb, Cr, Cd, and Ni are USEPA priority controlled pollutants (Wu et al., 2011). The smashed filters were digested at 170 °C for 4 h in high-pressure Teflon digestion vessel with 3.0 mL concentrated HNO_3, 1.0 mL concentrated $HClO_4$, and 1.0 mL concentrated HF. Afterwards, the almost dry solution was diluted and characterized using Inductively Coupled Plasma Optical Emission Spectrometer (ICP-OES, Atom Scan 2000, JarroU-Ash, USA). The following

wavelength lines of the ICP-OES analysis were used: As 189.042, Pb 220.353, Cd 228.802, Cr 205552, Ni 231.604, V 311.071, Zn 206.191, and Al 394.401. All reagents used were of highest grades, and recovery tests were conducted with standard additions, recoveries of each element were in the range of 93%~102% (see in SI, Table S2).

Another 1/4 of each filter was ultrasonically double extracted with 15.0 mL HPLC-grade CH_2Cl_2. The extracts were then condensed with rotary evaporator and quantified to 1.0 mL. 16 targeted PAHs (2-ring, naphthalene (Nap); 3-ring, acenaphthylene (Ac), acenaphthene (Ace), fluorene (Fl), phenanthrene (Phe), anthracene (Ant); 4-ring, fluoranthene (Flu), pyrene (Pyr), benzo[a]anthracene (BaA), chrysene (Chr); 5-ring, benzo[b]fluoranthene (BbF), benzo[k]fluoranthene (BkF), benzo[a]pyrene (BaP), dibenzo[a,h]anthracene (DBA); and 6-ring: indeno[1,2,3-cd] pyrene (IP), benzo[ghi]perylene (BghiP)) and 5 selected phenols (phenol, 2-methoxyphenol, 4-ethylphenol, 4-ethyl-2-methoxyphenol, 2,6-dimethoxyphenol) were measured from the concentrated extracts using an Agilent 6890 Series gas chromatography system coupled with a HP 5973 Mass Selective Detector (GC-MS, Agilent Technologies, Wilmington DE) . A DB-5ms (30 m × 0.32 mm × 0.25 mm, Agilent 123-5532) column was installed. The temperature programs were presented as follows: initially at 40 ^{o}C, hold for 4 min, to 150 ^{o}C at 20 ^{o}C min^{-1}, then to 280 ^{o}C at 5 ^{o}C min^{-1}, hold for 10 min. The interface temperature was kept at 280 ^{o}C, the MS was operated in electron impact mode with an ion source temperature of 230 ^{o}C, and the high-purity helium (99.999%) carrier gas was maintained at a constant pressure of 16.2 psi with a flow of 2.0 mL min^{-1}. The calibration curves were optimized to be better than 99.9%. Prior to the measurements, PAHs and Phenols recovery studies were undertaken, and recoveries were acceptable with rates of 82%~99% (see in SI, Table S2). In addition, Phenanthrene-d10 (Phe-d10) as internal standard surrogate was added into the PAHs mixture, recovery rate of which was 94%.

Organic carbon (OC) and elemental carbon (EC) were measured with the rest quartz filters using a carbon analyzer (Sunset laboratory Inc., Forest Grove, OR) based on the thermal-optical transmittance (TOT) method with a modified NIOSH-5040 (National

Institute of Occupational Safety and Health) protocol. Four organic fractions (OC1, OC2, OC3, and OC4 at 150, 250, 450, and 550 ^{o}C, respectively), PC fraction (a pyrolyzed carbonaceous component determined when transmitted laser returned to its original intensity after the sample was exposed to oxygen), and three EC fractions (EC1, EC2, and EC3 at 550, 700, and 800 ^{o}C, respectively) are produced. And OC is technically defined as OC1 + OC2 + OC3 + OC4 + PC, while EC is defined as EC1 + EC2 + EC3 - PC (Seinfeld et al., 2012). The instrument detection limits for total OC and EC that deposit on the filter are 0.25 and 0.12 μg C cm^{-2}. The quality of the data above was guaranteed by standard materials calibration, recovery rate, and operational blank correction. And blank levels were less than 5% of the measured values for all the species.

2.1.5 Calculation of emission factors

The emission quantities derived from the experiment were converted into quantities per unit weight of initial residues as emission factor (EF, unit: g kg-1), which can be calculated from the direct method with effective filter sampling weight, chamber volume, and effective amount of crop straw consumed (Dhammapala et al., 2006, 2007a, b; Zhang et al., 2008a), or alternatively from the carbon mass balance method (CMB) via conservation of Carbon in biomass, disregarding the weight of biomass that burnt (Dhammapala et al., 2006; Li et al., 2007). EFs determined from these two methods were found to be in good agreement (Dhammapala et al., 2006), nevertheless, CMB method needs more auxiliary information (e.g., concentrations of CO, CO_2, CH_4, non-methane hydrocarbons, and also particulate carbons), which may result in data redundancy and uncertainty propagation, hence we applied the direct method to calculate EFs in this work. To be more accurate, influence of wall loss and makeup air dilution on smoke particles sampling from the chamber were considered and corrected, details see in SI.

In this study, duration for each test (burning, chamber condition, size measurement, and filter sampling) was controlled within 20 min, therefore, the physicochemical

processes of pollutants in the chamber can be negligible, and smoke aerosols we measured were primary emissions.

2.2 Emission inventory calculation

2.2.1 Agricultural field fire survey

Fire sites over China from 2011 to 2013 were statistically analyzed, and the data of mainland agricultural fire sites was derived from the daily report of the Ministry of Environmental Protection of China (MEPC) (website: http://hjj.mep.gov.cn/jgjs/). Agricultural fire sites were screened out from MODIS (Moderate Resolution Imaging Spectroradiometer) daily fire products (1 km × 1 km resolution level 3 hotspot) using a high resolution real time land use based on geography information system (GIS). Spatial and temporal distributions of fire sites were displayed in Fig. S2 (SI), over 5000 fire sites were allocated into two prominent burning periods corresponding to summer (May to July) and autumn (September to November) harvests, and filed burning last 54 days and 60 days on statistical average during the two harvests. In the North of China, open burning occurred primarily in autumn, while temporal-character of field fires was not obvious in the North Plain and the Center of China, where field fires can be observed frequently during the whole investigation time.

2.2.2 Crop straw production

Crop straw production was generally derived from annul or monthly crop production by multiplying crop-specific ratios of residue-to-production (He et al., 2011b; Cao et al., 2011; Zhao et al., 2012). In this study, crop productions were furtherly classified into summer harvest and autumn harvest productions according to field fire sites analysis and traditional seasonal planting and harvesting. The amount of straw produced was calculated by Eq. (3):

$$M_{t,k,i} = P_{t,k,i} \times r_i \times H_{t,k,i} \times D_i \quad (3)$$

in which M is mass of crop straws produced; P is annual crop-specific amount of crop

372 production; r is the residue-to-production ratio; D is the dry matter content; $H_{t,k,i}$ is
373 production ratio of crop i at region k during summer or autumn harvest period t.
374 Province-level crop production data of wheat, rice, corn, cotton, and soybean were
375 taken directly from the China Yearbook 2013 (National Bureau of Statistics of China,
376 NBSC, 2013). Crop-specific residue-to-production ratios were cited from Chinese
377 Association of Rural Energy Industry (Wang and Zhang, 2008; data available at
378 http://www.carei.org.cn/index.php, in Chinese). Dry matter contents of crop straws
379 were referred to He et al. (2011b) and Greenhouse Gas Inventory Reference Manual
380 (IPCC, 2007). The parameters of residue-to-production ratios and dry matter contents
381 were summarized in Table S3 (SI). The regional crop production ratios in summer and
382 autumn harvests were listed in Table S4 (SI).

383 **2.2.3 Field burning rate**

384 Uncertainty of emission estimations mostly relies on intangibility of straw open
385 burning rate (Zhao et al., 2012; He et al., 2011b). However, regional or national
386 percentage of straw open burned was seldom studied, and the limited data were
387 outdated and variable. The available studies indicate national filed burning rate of
388 crop straws range from 15.2% to 27.2% in China (Daize, 2000; Wei et al., 2004;
389 Zhang et al., 2008a), and more detailed studies indicate about 31.9% of the crop straw
390 burned in the Pearl River Delta from 2003 to 2007 (He et al., 2011b), while the
391 corresponding figures were almost 100% for the Huabei region in 2003 (Zhao et al.,
392 2012). Two versions of province-level field burning rates were commonly used, one
393 was from Cao et al. (2005; 2006; 2011) who deduced the rates based on regional
394 economic level, and the proposal of the rates to be proportional to peasants' income
395 was confirmed later, the rates were first used to calculate open burning emission in
396 2000. The other version was reported by Wang and Zhang (2008), they obtained
397 provincial percentage of residue open burnt via filed survey in 2006. Herein, the two
398 versions were both applied directly into the emission estimation of 2012 in this work
399 and named as business-as-usual scenarios (BAU, BAU-I from Cao et al. and BAU-II

400 from Wang and Zhang in specific).

401 In fact, the burning rates should be dynamic parameters that been influenced by
402 industrial structure, government policy orientation, or public awareness. With crop
403 yields increase and energy consumption structure changes in rural areas, more straws
404 will be discarded and burnt in the field. Nonetheless, rigorous agricultural fire policy
405 may still suppress the condition worsen as it worked during 2008 for Beijing
406 Olympics and 2010 for Shanghai Expo (Huang et al., 2013; Cermak and Knutti, 2009;
407 Wang et al., 2010). Qin and Xie (2011; 2012) ever deduced year specific open burning
408 rates in different zone for the period of 1980-2009 according to their respective
409 peasant income changes in a certain year on the basis of peasant income and burning
410 rates in 2006. However, the simple linear relationship should be doubted, as great
411 increase in per capita income after 2006 will surely overestimate the burning rates. We
412 supposed that the burning rates were inverse proportional to peasants' agricultural
413 income proportion (AIP), without considering the policy or potential gain or loss
414 related to agricultural residue treatment. Thus the burning rates established in 2000
415 and 2006 from Cao et al. (2005) and Wang and Zhang (2008) can be converted into
416 that of 2012 based on economic data from equation below:

417 $$R_{k,2012} = \frac{I_{k,2012}}{AI_{k,2012}} \times \frac{AI_{k,y}}{I_{k,y}} \times R_{k,y} \quad (4)$$

418 where R is agricultural straw filed burnt rate, $I_{k,y}$ is peasants' annual income, $AI_{k,y}$ is
419 peasants' annual agricultural income. y indicates reference year (2000 for BAU-I, and
420 2006 for BAU-II). $I_{k,y}$ and $AI_{k,y}$ can be found or calculated from China Yearbook
421 and China Rural Statistic Yearbook (NBSC, 2004-2013).

422 The versions of converted rates based on primary industry level were called
423 Economic Models I and II (EM -I and EM-II in short) corresponding to BAU-I and
424 BAU-II. Besides, in 2013, the National Development and Reform Commission of
425 China published the Chinese agricultural straw treatment report of 2012 (NDRC,
426 [2014] No.516, data available at http://www.sdpc.gov.cn/, in Chinese) for the first
427 time. The percentages of crop residues discarded in the report were applied in our
428 estimation, which was called NDRC version.

2.2.4 Emission and flux concentration

From above study, emission of SPM pollutants can be calculated by recount of Eq. (1) to get Eq. (5) as it was showed below:

$$E_{t,k,j} = \sum_i M_{t,k,i} \times R_k \times f_i \times EF_{i,j} \quad (5)$$

where $E_{t,k,j}$ is emission amount of chemical species j at region k during harvest period t; f_i is burning efficiency, the crop specific values were cited as 0.68 for soybean residue and 0.93 for the rest four straws (Zhang et al., 2011; Wang and Zhang, 2008; Zhang et al., 2008a; Koopmans et al., 1997). Thus, flux concentration of corresponded pollutants can be also assessed from box model as mentioned in front.

2.3 Estimate health impacts and health-related economic losses

2.3.1 Carcinogenic risk of Smoke Particulate Matter (CR_{SPM})

Apart from the enormous climatic effects of smoke particle emissions, new epidemiological and toxicological evidence have also linked carbonaceous aerosol to cardiovascular and respiratory health effects according to the World Health Organization (Bruce et al., 1987; IPCC, 2007). Here, we present the fuel-specific carcinogenic risk of SPM (CRSPM, unit: per μg m^{-3}) to assess health hazard from agricultural straw burning particles and help source-specific air quality control. The cancer risk attributed to inhalation exposures of smoke $PM_{2.5}$ from crop straw i burning was calculated as:

$$CR_i = \sum_j f_j \times UnitRisk_j \quad (6)$$

where f_j is mass fraction of individual species j in smoke $PM_{2.5}$, $UnitRisk_j$ is corresponded unit carcinogenic risk value of species j extracted from database provided by the Integrated Risk Information System (IRIS), California Environmental Protection Agency (CEPA), and related documents (Bruce et al., 1987; Burkart et al., 2013; Tsai et al., 2001; Wu et al., 2009, 2011).

CR_i is estimated based on dose addition model of selected hazardous air pollutants

(HAPs) including USEPA priority pollutants of PAHs and heavy metals. And UnitRisk values of the selected HAPs presented in Table S5 (SI). Synergistic interactions among pollutants are dismissed, albeit possible. The cancer risk of chromium is adjusted by multiplying a factor of 0.2, assuming that only 20% Cr measured is in the toxic hexavalent form (Bell and Hipfner, 1997). Benzo[a]pyrene (BaP) is used as an indicator compound of carcinogenicity, legally binding threshold of BaP in most countries ranges from 0.7 to 1.3 ng m^{-3}, corresponded carcinogenic risk of BaP is about 1.1×10^{-6} per ng m^{-3} (Bruce et al., 1987; Burkart et al., 2013). Thus, one in million level of carcinogenic potential is frequently used to identify risks of concern in public health and environmental decision making, and permissible exposure limits (PEL, unit: μg m^{-3}) of crop straw burning particles can be estimated as:

$$\mathrm{PEL_i} = \frac{10^{-6}}{\mathrm{CR_i}} \quad (7)$$

2.3.2 Human exposure and health impacts

Robust relationship between surface $PM_{2.5}$ and health effects has been revealed and confirmed by many studies (Pope et al., 2004; Wong et al., 2008). $PM_{2.5}$-related health endpoints are composed of a range of elements from sub-clinical effects to the onset of diseases and the final death (Davidson et al., 2005). In this study, incidence of commonly studied endpoints like premature mortality, respiratory and cardiovascular hospital admissions, and chronic bronchitis from primary emitted smoke $PM_{2.5}$ short-term exposure were assessed using the Poisson regression model, shown as below (Guttikunda and Kopakka, 2014):

$$\Delta E = \Delta Pop \times IR \times \left(1 - \frac{1}{e^{\beta\times\Delta C}}\right) \quad (8)$$

where ΔE represents the number of estimated cases of mortality and morbidity, ΔC is the incremental concentration of particulate matter (PM) or flux concentration; ΔPop is the population exposed to the incremental particulate concentration of ΔC; IR is short for incidence rate of the mortality and morbidity endpoints, and β is the coefficient of exposure-response function, defined as the change in number case per unit change in concentration per capita.

Concentration-response function and incidence rate of each health endpoint are important in health impacts evaluation and they have variation for different population and regions (Yang et al., 2012; Wong et al., 2008). Here, the variance for sex and ages were neglected. Region-specific exposure-response coefficients for individual mortality were summarized from previous studies, as presented in Table S6 (SI). The coefficients for individual respiratory and cardiovascular hospital admission, and chronic bronchitis were cited as 1.2%, 0.7%, and 4.4% (per 10 μg m^{-3}, 95% CI) from Aunan and Pan's work (Aunan and Pan, 2004). This is the case because seldom studies ever confirmed these topics in China. Region-specific mortality and hospitalization IRs were taken from statistical reports authorized by National Health and Family Planning Commission of the People's Republic of China (NHFPC, 2013), and morbidity of chronic bronchitis were defined as 13.8 ‰ based on the forth national health survey, which was released by the Chinese Ministry of Health in 2008 (CMH, 2009).

2.3.3 Economic valuation of the health impacts

The economic losses of the health impacts associated with smoke $PM_{2.5}$ exposure in 2012 were further evaluated. The amended human capital (AHC) approach was employed to calculate the unit economic cost of premature mortality. The commonly applied AHC method uses per capita GDP to measure the value of a statistical year of life (IBRD and SEPA, 2007) based on Eq. (9). It can be used as a social statement of the value of avoiding premature mortality and estimates human capital (HC) from the perspective of entire society, neglecting individual differences (Hou et al., 2012).

$$HC_k = \frac{GDP_k}{POP_k} \times \sum_{i=1}^{\tau} \frac{(1+\alpha)^i}{(1+\gamma)^i} \quad (9)$$

GDP_k and POP_k are gross domestic production and population of target region k that were reported in the statistical yearbook in 2012; α and γ are economic parameters referring to national GDP growth rate and social discount rate, which were 7.7% and 8.0% in 2012 from National Bureau of Statistics of China (NBSC, 2013, data available at http://www.stats.gov.cn/tjsj/ndsj/, in Chinese). τ is the

life-expectancy lost due to aerosol pollution, and 18 years of life was widely applied (Hou et al., 2012). The annual exchange rate of US dollar to RMB was 6.31 in 2012. One can deduce the HC values of the provinces, municipalities, and autonomous regions in the country, and the calculated regional HC values were listed in Table S7 (SI). In this paper, the cost of respiratory, cardiovascular hospital admissions, and chronic bronchitis were 632.2, 1223.4, and 948.6 US$ per case in 2012, which were derived from the national health statistical reports (NHFPC, 2013).

The regional and national health-related economic loss from smoke $PM_{2.5}$ exposure can be calculated based on the excess mortality and morbidity multiplied by the corresponding unit economic values.

3 Result

3.1 Particulate chemical compositions and emission factors

3.1.1 Organic carbon and elemental carbon

An overview of particulate chemical compositions for smoke $PM_{2.5}$ and $PM_{1.0}$ is pie-graphically profiled in Fig. 2, and the corresponded emission factors are given in Table 1-2 (detailed EFs for elements, PAHs, and Phenols in Table S8 and S9, SI). From multivariate statistical analysis ($P<0.05$ at 95% CI), significant differences of chemical compositions and emissions in size range and fuel types can be observed, implying the nonuniform mixing and distribution of particulate pollutants from biomass burning, which is consistent with the conclusion from Lee et al. (2015) and Giordano et al. (2015). EFs of particulate species from this study were compared with that from literature as summarized in Table 3, since EFs in smoke $PM_{1.0}$ were seldom reported, only smoke $PM_{2.5}$ or total particulate matter emissions were collected, which were comparable with the results in this work. EFs of smoke $PM_{2.5}$ and $PM_{1.0}$ were in range of 3.25~15.16 and 3.04~13.20 g kg^{-1} for the five kinds of crop straws, a high ratio of $PM_{1.0}/PM_{2.5}$ was observed to be over 90 wt.%, which was in line with size distribution analysis of smoke particles given in Fig. S3 (SI). Li et al. (2007) measured

the emissions from field burning of crop straws via CMB method, $PM_{2.5}$ EFs for wheat and corn straw were estimated to be 7.6±4.1 and 11.7±1.0 g kg^{-1} (dry basis, MCE > 0.9), which were higher and presented more uncertainties than our result. As study ever found a positive relationship between particulate EFs and moisture content of agricultural residue (Hayashi et al., 2014), it was reasonable that combustion of the dehydrated crop straw produced less smoke aerosol in this work. Hayashi et al. (2014) measured particulate EFs to be 2.2 and 15.0 g kg^{-1} for rice and wheat straw of ~10 wt.% moisture content, while corresponded EFs increased to 9.1 and 19.5 g kg^{-1} when water content of straw was ~20 wt.%, and the linear equations between smoke EFs and straw moisture content were furtherly proposed. However, the simple linearity and its application scope should be doubted, as Hayashi et al. only considered two water content levels (10 wt.% *vs* 20 wt.%) and disregarded influence of combustion efficiency for the fires. $PM_{2.5}$ EFs given by Dhammapala et al (2006, 2007a, b) were 4.7±0.4 g kg^{-1} for wheat straw and 12.1±1.4 g kg^{-1} for herbaceous fuel that were burnt using a chamber under flaming phase, and negative response for particulate EFs to combustion efficiency was observed. After all, smoke EFs vary with fires depend on fuel type and moisture, combustion phase, environmental conditions, and some other variables (Reid et al., 2005b).

The carbonaceous materials (Organic matter and EC) are dominated in SPM, accounting for about 73.4 wt.% for $PM_{2.5}$ and 71.3 wt.% for $PM_{1.0}$ on average. Organic matter (OM) was converted from OC by multiplying a factor of 1.3 to account for noncarbon materials like oxygen, hydrogen, and other minor species (Li et al., 2007; Li et al., 2015), and Li et al. (2016) ever measured OM/OC ratio as ~1.3 for fresh smoke particles via volatility analysis. EFs of EC and OC from this work were consistent with most studies, average OC EFs were 4.21 and 3.58 g kg^{-1} in smoke $PM_{2.5}$ and $PM_{1.0}$, and the corresponded EC EFs were 1.09 and 1.01 g kg^{-1}, respectively. These values fell within the ranges (0.9~9.3 g kg^{-1} for OC and 0.2~1.7 g kg^{-1} for EC) found in other similar sources (Dhammapala et al., 2007; Hayashi et al., 2014; Li et al., 2007; May et al., 2014). Due to the technical limitation and ambiguous artificial boundary, carbon contents of biomass burning particles have vast variability and

uncertainty (Lavanchy et al., 1999; Levin et al., 2010). It was ever reported chamber burn study may overestimate EC EFs due to a misassigned OC-EC split for the heavily mass loaded filter samples (Dhammapala et al., 2007b). Moreover, carbon measurement based on TOT method with NIOSH protocol may overestimate OC fraction by sacrificing EC part compared with that of TOR (Thermal-Optical Reflectance) method with IMPROVE program (Han et al., 2016). Mass ratio of OC/EC is a practical parameter to indicate the primary organic aerosol (OA) emission and secondary organic aerosol (SOA) production. The ratio is influenced by burning conditions, source, aging extent, and particle size (Engelhart et al., 2012; Grieshop et al., 2009). Smoke emitted from smoldering fires is OC-dominated while flaming combustion produces more EC, and the discrepancy of OC/EC ratio can be an order of magnitude regarding to different combustion phase (Grieshop et al., 2009). SOA production upon photo-oxidation will enlarge OC/EC ratio, and positive relation between oxidation level of OA loading and OC/EC ratio was reported (Grieshop et al., 2009). Here, OC/EC ratio in primary emissions varied from 2.4 to 6.2 under flaming phase, similar to previous studies (Arora and Jain, 2015; Dhammapala et al., 2007a, b; Hayashi et al., 2014; Lewis et al., 2009). The OC/EC ratios were larger in $PM_{2.5}$ with average value of 3.8, while it was 3.6 in $PM_{1.0}$, indicating more EC resides in $PM_{1.0}$.

3.1.2 Water soluble organic acids

Smoke particles comprise a considerable amount of water soluble organic acids (WSOA), it was 3.35 wt.% in $PM_{2.5}$ and 3.17 wt.% in $PM_{1.0}$ on average, which was in line with previous work that organic acids measured represent less than 5 wt.% of the total smoke aerosol mass load and favor to partition in larger size (Falkovich et al., 2005; Gao et al., 2003). Acetic acid followed by methysulfonic acid contributed the most of the measured low molecule weight acids. Oxalic acid is the dominated dicarboxylic acids measured in the ambient environment and biomass burning aerosol (Falkovich et al., 2005; Kundu et al., 2010), and oxalic acid EF was measured to be 2.2 ~ 4.8 and 1.6 ~ 3.6 mg kg^{-1} for smoke $PM_{2.5}$ and $PM_{1.0}$ in present work. The sums of

WSOA EFs ranged from 46.7 to 770.0 mg kg^{-1}. Correlation among the multi-pollutants was analyzed by relevance matrix as shown in Table S10 (SI), the strong positive linear relationship (R^2>0.99, p<0.05 at 95% CI) between WSOA and emissions of OC and PM was observed. Study has confirmed organic acids contribute a significant fraction of both oxygenated volatile organic compounds (OVOCs) in gaseous phase and SOA in particulate phase, the direct emission of particulate organic acids from biomass burning also represents a significant source of precursors for SOA formation, as the low molecular organic acids will evaporate into gas phase or involve in the heterogeneous reaction directly (Takegawa et al., 2007; Veres et al., 2010; Yokelson et al., 2007; Carlton et al., 2006). Moreover, as the significant fraction of water soluble organic carbon, organic acids play major response to CCN activity of smoke particles, and organic acids coating or mixing can amplify hygroscopic growth of inorganic salts by decreasing the deliquescence RH, enable the particle to be CCN at relative low degree of supersaturation (Falkovich et al., 2005; Ghorai et al., 2014). In the ambient environment, organic acids can enhance atmospheric new particle formation by impairing nucleation barrier (Zhang et al., 2004), besides, particulate organic acids can also mobilize the solubility of mineral species, like iron, altering the chemical process of particles (Cwiertny et al., 2008). And prominent optical properties of organic acids like humic/fulvic substance make them as potential contributors to the global warming (Yang et al., 2009; Andreae and Gelencsér, 2006).

3.1.3 Water soluble aminiums

Interest has been focused on the vital role of amines in particle nucleation-growth process and acidity regulating due to their strong base (Tao et al., 2016; Bzdek et al., 2010, 2011). Though ultratrace gaseous amines and particulate aminiums were on the order of pptv or ng m^{-3}, aminium salts exhibit potential climatic and health effect due to their significant different properties in hygroscopicity, optics, and also toxicology (Qiu and Zhang, 2012; Qiu et al., 2011; Samy and Hays, 2013; Zheng et al., 2015; Ho et al., 2015; Tao et al., 2016). It ever proposed that biomass burning is an important

source for gaseous amines, especially from smoldering burning, and alkyl amides can be served as biomarkers in particular (Ge et al., 2011; Ho et al., 2015; Lee and Wexler, 2013; Lobert et al., 1990; Simoneit et al., 2003). However, seldom study ever quantitatively explored the particulate water soluble amine salts (WSA) in primary smoke emissions (Schade and Crutzen, 1995; Ge et al., 2011). From this study, WSA contributed about 4.81 wt.‰ of smoke $PM_{2.5}$ and 4.69 wt.‰ of $PM_{1.0}$, implicating aminium favored to be abundant in fine-mode of smoke particles, especially in $PM_{2.5-1.0}$. $DEAH^+$, $TMAH^+$, $TEOH^+$ and $DMAH^+$ made up over 80 wt. % of the measured WSA. Fuel-dependence of WSA distribution and emissions were evident. EFs of WSA ranged from 4.5 to 104.8 mg kg^{-1} in smoke $PM_{2.5}$, the least was from burning of soybean straw and the largest from cotton and rice straws. We used mass ratio of WSA to NH_4^+ to denote the enrichment of aminium in particulate phase. Statistical analysis showed WSA/NH_4^+ was 0.16 ± 0.03 and 0.18 ± 0.06 in smoke $PM_{1.0}$ and $PM_{2.5}$, respectively, which were almost one order of magnitude larger than that in the ambient aerosol (Liu and Bei, 2016; Tao et al., 2016). Tao et al. (2016) ever measured the ratio as a function of particle size during NPF days in Shanghai, and a noticeable enrichment of aminiums for ultrafine particles (<56 nm) was observed with WSA/NH_4^+ over 0.2, highlighting the competitive role for amines to ammonia in particle nucleation and initial growth of the nuclei, the ratio was then decreased with the increasing particle size, and the final increasing trend was found after ~ 1.0 μm, and average WSA/NH_4^+ for ambient bulk $PM_{1.0}$ and $PM_{2.5}$ were 3.2% and 3.5% , respectively.

3.1.4 PAHs and Phenols

Atmospheric PAHs are primarily the byproduct of incomplete combustion of biomass and fossil fuels (Simcik et al., 1999; Galarneau, 2008). Due to their high degree of bioaccumulation and carcinogenic or mutagenic effect, the sources and environmental fate of the ubiquitous PAHs have been the subjects of extensive studies (Santodonato, 1997; Kim et al., 2013). PAHs can involve in photochemical reaction to form SOA,

the process is influenced by gas-to-particle partition and meteorological conditions. Moreover, oxidation may increase the toxicity of PAHs (Arey and Atkinson, 2003; Wang et al., 2011). Biomass burning is one of the main sources of gaseous and particulate PAHs, which even contributes to about half of anthropogenic PAHs emissions in China (Xu et al., 2006; Zhang et al., 2011). Burning conditions can significantly influence the emission of PAHs, under the flaming phase in this study, PAHs contributed 0.46 wt.‰ of smoke $PM_{2.5}$ and 0.28 wt.‰ of $PM_{1.0}$, over 60% of the total PAHs were associated to respiratory submicron particles. The sum of EFs of 16 PAHs in smoke $PM_{2.5}$ ranged from 1.81 to 8.30 mg kg^{-1}, which were consistent with the values from literature (Dhammapala et al., 2007a, b; Lee et al., 2005; Zhang et al., 2011). Hays et al. (2005) estimated total EFs of 16 PAHs to be 3.3 mg Kg^{-1} in wheat straw burning $PM_{2.5}$. Korenaga et al. (2001) measured PAHs EFs from rice straw burning to be 1.9 mg Kg^{-1} in particulate phase, while the value from Jenkins et al. (1996) was 16 mg Kg^{-1}. Dhammapala et al. (2007b) found negative linear response for biomass burning source PAHs emissions to burning efficiency, and under flaming combustion, particulate total 16 PAHs EFs were 2 ~ 4 mg Kg^{-1}. Zhang et al. (2011) simulated burning of rice, corn, and wheat straws, the corresponded PAHs EFs were measured as 1.6, 0.9, and 0.7 mg Kg^{-1} in fine smoke particles, respectively. Great uncertainties for PAHs EFs were evident that relied on burning phase, fuel types, moisture content, and also measurement techniques. Dhammapala et al. (2007a) also found laboratory simulation might overestimate the emission factors of PAHs compared with field burnings. EFs for individual PAHs were included in Table S8 and S9 (SI). The distribution of particulate PAHs emission factors was presented in Fig. 3a. Of the particle bound PAHs, 3~4-rings components were the primary ones, including Pyr, Ant, Ace, Flu, Phe, and Chr. Concentration ratios of selected PAHs, namely diagnostic ratios, were usually used to trace the source and make apportionment of specific pollutions (Yunker et al., 2002; Simcik et al., 1999). In this work, average Ant/(Ant+Phe), Flu/(Flu+Pyr), BaA/(BaA+Chr), and IP/(IP+BghiP) ratios of 5 types agricultural residue burning smokes were 0.72, 0.36, 0.47, and 0.58, respectively. There was no significant difference ($P<0.05$ at 95% CI) of the ratios in $PM_{1.0}$ and

682 $PM_{2.5}$. According to previous work, Ant/(Ant+Phe) above 0.1 and BaA/(BaA+Chr)
683 above 0.35 indicate the dominance of combustion and pyrolytic sources, Flu/(Flu+Pyr)
684 and IP/(IP+BghiP) ratios greater than 0.50 suggest coal or biomass burnings dominate
685 (Simcik et al., 1999; Yunker et al., 2002). However, validation of source
686 apportionment using specific diagnostic ratios should have its constraints, because of
687 variations in source strengths and atmospheric processing of PAHs (Arey and
688 Atkinson, 2003; Galarneau, 2008).

689 From Table S10 (SI), PAHs in smoke particles were highly correlated with EC and
690 OC contents. PAHs primarily originate from pyrolysis of organic materials during
691 combustion, and formation mechanisms of PAHs and soot are closely intertwined in
692 flames. High-molecular-weight PAHs (>500 atomic mass unit) act as precursors of
693 soot particles (Lima et al., 2005; Richter et al., 2000). Thus, PAHs with 3, 4, and 5
694 rings accumulate and dominate in the emissions of biomass burning, as larger
695 molecular weight PAHs tend to incorporate into soot particles. PAHs
696 expulsion-accumulation in OC and EC fractions were analyzed by linear fitting of
697 PAHs mass fractions and EC mass fractions in carbonaceous materials (EC+OC) in
698 Fig. 3b. The partitions can be parameterized as Eq. (10):

699 $$f_{PAHs} = \frac{m_{PAHs}}{m_{OC}+m_{EC}} = \beta_{EC} \times \frac{m_{EC}}{m_{OC}+m_{EC}} + \beta_{OC} \times \frac{m_{OC}}{m_{OC}+m_{EC}} = \beta_{EC} \times f_{EC} + \beta_{OC} \times f_{OC} \quad (10)$$

700 where f_{EC} and f_{OC} are the mass fraction of OC and EC in carbonaceous materials
701 (EC+OC). β_{EC} and β_{OC} are expulsion-accumulation coefficients of PAHs in OC and
702 BC. The coefficient of β_{EC} is 1.1×10^{-3} in smoke $PM_{1.0}$ and 1.9×10^{-3} in $PM_{2.5}$, the
703 corresponded β_{OC} is 0.3×10^{-3} and 0.5×10^{-3}.

704 Phenols are the most common SOA precursor/product and organic pollutants in the
705 atmosphere (Berndt and Böge, 2006; Schauer et al., 2001). Hydroxyl functional group
706 and aromatic benzene ring make phenols a paradigm in heterogeneous reaction upon
707 photo oxidation research and aqueous phase reaction research. Phenols are also ROS
708 (reactive oxidized species) precursors that present health hazard (Bruce et al., 1987).
709 Phenol and substituted phenols are thermal products of lignin pyrolysis during
710 biomass burning (Dhammapala et al., 2007a), and the most abundant methoxyphenols

711 can be markers of biomass burning sources (Urban et al., 2016). The five measured
712 phenols contributed 3.0 wt.‰ and 2.5 wt.‰ of $PM_{2.5}$ and $PM_{1.0}$. 2,
713 6-dimethoxyphenol was the major one of the measured phenols. Mass fraction of
714 phenols was about 7~9 times of PAHs in smoke aerosols. EFs for the sum phenols
715 were 9.7 ~ 41.5 and 7.7 and 23.5 mg Kg^{-1} for smoke $PM_{2.5}$ and $PM_{1.0}$, respectively.
716 Dhammapala et al. (2007a) estimated particulate methoxyphenols emissions to be 35
717 ± 24 mg Kg^{-1} for wheat straw burning, while Hays et al. (2005) measured the same
718 compounds to be 6.8 mg Kg^{-1}. Carbonaceous materials like PAHs and Phenols or
719 aromatic and phenolic deviates are the main chromophores in the atmosphere, and the
720 considerable fractions of PAHs and Phenols justify biomass burning as a significant
721 source of brown carbon (Laskin et al., 2015), study has proved ~ 50% of the light
722 absorption in the solvent-extractable fraction of smoke aerosol can be attributed to
723 these strong BrC chromophores (Lin et al., 2016).

724 **3.1.5 Inorganic components**

725 From Fig. 2, smoke particles consisted of approximately 24 wt.% water soluble
726 inorganics (WSI), and the inorganic salts resided more in submicron particles. Great
727 amount of inorganics enable smoke particles to be efficient CCN, and the distinct
728 optical scattering characters of the inorganic fractions may neutralize the warming
729 effect of brown carbon for smoke aerosol, otherwise, inorganics coating or mixing
730 will enhance light absorbing of BC. K^+, NH_4^+, Cl^-, and SO_4^{2-} were the principle
731 inorganic ions. Particulate enriched K^+ together with levoglucose are treated as tracer
732 of pyrogenic source (Andreae et al., 1998). And specific mass ratio of K^+/OC or
733 K^+/EC will help make source apportionment of particulate pollutants with PMF
734 (Positive Matrix Factorization) and PFA (Principle Balance Analysis) models (Lee et
735 al., 2015). K^+/OC in smoke particles ranged from 0.11 to 0.25 with average value of
736 0.17 in $PM_{1.0}$ and 0.14 in $PM_{2.5}$, which were similar to those reported for the Savannah
737 burning and agricultural waste burning emissions in India and China (Echalar et al.,
738 1995; Ram and Sarin, 2011; Li et al., 2015). However, OC represents large uncertainty

arise from degree of oxidization and burning condition, K^+/EC is more practical parameter to distinguish the pyrogenic pollutants in ambient study. To smoke particle emitted from flaming fires, K^+/EC was 0.58 ± 0.24 in $PM_{1.0}$ and 0.53 ± 0.18 in $PM_{2.5}$. Cl^- was the main anion to balance the charge of WSI in smoke particles. Mean charge ratio of Cl^- : K^+ was 1.46 and 1.49 in $PM_{1.0}$ and $PM_{2.5}$, implicating surplus chloride will associate with other cations. With atmospheric aging, the Cl/K ratio will decrease as chloride being replaced by secondary sulfate and nitrate (Li et al., 2015; Li et al., 2003). Equivalent charge ratio of primary cations (NH_4^+ + K^+) to primary anions (SO_4^{2-} + Cl^-) was 1.05 in $PM_{1.0}$ and 1.01 in $PM_{2.5}$ on average, and charge ratios of total cations to anions ($R_{C/A}$) was 1.09 and 1.07 in $PM_{1.0}$ and $PM_{2.5}$. $R_{C/A}$ was used to indicate the neutralizing level of particulate matters in many studies. $R_{C/A} \geq 1$ indicates most of the acids can be neutralized, while $R_{C/A} < 1$ means atmospheric ammonia is deficient and the aerosol is acidic (Adams et al., 1999; He et al., 2011a; Kong et al., 2014). In ambient environment, acidic aerosol was prevailing urban pollutants in many cities from field investigation (He et al., 2011a; Kong et al., 2014). Acidic aerosols can increase the risks to human health and affect the atmospheric chemistry by activating hazardous materials and promoting the solubility of particulate iron and phosphorus (Amdur and Chen, 1989; Meskhidze, 2005). The emission and transport of biomass burning particles may neutralize the acidity of ambient particles. However, only limited WSI were brought into in the analytical system, it is not really to tell the acidity or base of smoke particles, considering the existence of massive organic acids and ammniums.

Trace mineral elements attracted great attention for the role as catalyst in atmospheric heterogeneous reaction and health cares (Davidson et al., 2005; Dentener et al., 1996). Wet/dry deposition of particles during long range transport will affect the ecological balance by releasing mineral elements (Jickells et al., 2005). Dust storm, weathering, and industrial process are the main sources of particulate metals, and incineration can also produce a lot of mineral elements (Moreno et al., 2013). However, the emissions of trace metals from biomass burning are highly uncertain (Li et al., 2007; Zhang et al., 2012), the great influence from local soil environment and

soil heavy metal pollution will certainly affect the metal content in biomass fuel and smoke particle. In this study, THM resided more in $PM_{2.5}$ than in $PM_{1.0}$. Smoke $PM_{2.5}$ consisted of 6.7 wt.‰ THM on average, $PM_{1.0}$ comprised 4.1 wt.‰ THM. Average EFs of THM in $PM_{2.5}$ and $PM_{1.0}$ were 0.056 g kg^{-1} and 0.028 g kg^{-1} in this work, of which Al contributed over 90 wt.‰, in line with result from domestic burning of wood and field investigation of crop straw burning (Li et al., 2007; Zhang et al., 2012). Smoke particles from wheat, rice, and corn straws contained more mineral elements than that from cotton and soybean residues combustion. Regardless the difference in biomass fuels, the result may imply that soil heavy metal pollution is heaver in the East China than that in Xinjiang in the West North of China (Wei and Yang, 2010).

3.2 Size, morphology, and mixing state of smoke particles

Fresh smoke particles exhibited unimodal size distribution within 500 nm (Fig. S3, SI), and previous chamber study has also confirmed that agricultural fire produces large amount of ultrafine particles, implying the great potential role to act as CCN and more profound threat to human health (Araujo et al., 2008; Delfino et al., 2005; Zhang et al., 2011). However, the role of particles in the atmospheric process and health hazard depends not only size, but also morphology and chemical mixing states (Dusek et al., 2006; Kennedy, 2007; Mikhailov et al., 2006; Schlesinger, 1985). From TEM images in Fig. 4, agricultural straw burning aerosols comprised a broad class of morphological and chemically heterogeneous particles. Non-uniformly internal mixing of the agglomerates was noticeable, including the major carbonaceous particles and a considerable amount of inorganic salt particles, which was consistent with previous particulate chemical analysis. KCl particles containing minor sulfate or nitrate were the primary inorganic particles, which presented crystal or amorphous state from X-ray diffraction analysis (Fig. 4 a, b, c). And potassium-bearing particles have been used as a tracer of ambient biomass burning pollutants. Fly ash particles were arresting due to visible morphology difference and mineral chemical composition (Fig. 4 d, e, f). Fly ash particles were more compact and rich in mineral

elements like Ca, Si, Fe, Al, Mn, and Cr. Besides, these particles had larger size, statistical average diameter of fly ash particles obtained from bulk analysis was 2.2 ± 1.6 μm. The result also proved heavy metals resided more in $PM_{2.5}$ than $PM_{1.0}$. Fly ashes are by products of incineration process (Buha et al., 2014), including coagulation of fuel issue debris, condensation of evaporated mineral metal from biomass fuels or adhered dirt at different burning phase. These fly ashes coated by or agglomerated with carbonaceous materials were like mash of mineral without clear lattice. Tar ball as a specific form of brown carbon and soot were representative particles of biomass burning aerosol (Wilson et al., 2013; Chakrabarty et al., 2010; Tóth et al., 2013). From Fig. 4 g, chain-like soot particles were coagulated with tar ball. Soot particles were agglomerates of small roughly spherical elementary carbonaceous particles, these chemical consistent particles were within 20~30 nm, and high-resolution TEM showed the soot spheres consisted of concentrically wrapped graphitic layers, while monomeric tar balls possessed disordered microstructure. Tar balls and soot corresponded to different stages in the aging of organic particles; tar balls abundant in fresh or slightly aged biomass smoke are formed by gas-to-particle conversion of high-molecular weight organic species or from aged primary tar droplets upon biomass burning. Soot represents further aged carbon-bearing particles, formed from the pyrolysis of lignin, cellulose, or tar balls (Pósfai, 2004; Tóth et al., 2013). The botryoid aggregates in Fig. 4 g can be viewed as transformation of tar ball to soot. Tar ball and soot were also internal mixed with inorganic salt including sulfate and nitrate (Fig. 4 g, h, i), which made the physiochemical properties of BC even complicated, as study has confirmed inorganic sulfate mixing will enhance light absorption and hygroscopicity of BC (Zhang et al., 2008b). Dark-ring like shell of tar ball (Fig. 4 g, h) and spot-like particles adhered to the surface of tar ball (Fig. 4 i) were K-rich materials. And size of soot particles was mainly within 200 nm, while tar ball and other carbonaceous particles can be over one micrometer.

824 **3.3 Open burning emissions**

825 **3.3.1 Crop straw production**

826 The agricultural straw productions were calculated and geographically displayed in
827 Fig. 5 a-c. Totally 647.3 Tg agricultural straws were produced in 2012 and dispersed
828 mainly in the North and Northeast of China. The distributions of the straws clearly
829 correspond to the distinct planting regions that are divided by Qinling
830 Mountain-Huaihe River line and the Yangtze River. Rice is primarily planted in the
831 south of Qinling Mountain-Huaihe River line, only 10 % rice (single cropping rice
832 dominate) is planted in Heilongjiang, Jilin, and Liaoning province, while wheat and
833 corn are grew mostly in the north of the Yangtze River. Over 90 % of the wheat
834 planted in China is winter wheat that gets ripe in summer, and more than 80 % rice
835 including middle and late rice grows mature in autumn. Summer harvest contributed
836 about 25 % of the agricultural straw production, which solely consists of rice and
837 wheat straws in this period and distributes uniformly in the central and east of China.
838 493.9 Tg crop straws were produced mainly from corn and rice harvesting in autumn.
839 Soybean and cotton straws account for about 8.6 % of autumn straw production that
840 were primarily produced in Heilongjiang and Xinjiang province.

841 **3.3.2 Open burning rate**

842 The five scenarios of field burning rates and regional AIP ($\frac{I_{k,y}}{AI_{k,y}}$) in the year of 2000,
843 2006, and 2012 were listed in Table 4 and statistically analyzed in Fig. 6. A significant
844 difference ($P<0.05$ at 95% CI) of regional burning rates among the versions was
845 observed, and the rates from NDRC report were generally higher. For convenience,
846 six zones were classified by geographic divisions and economic areas in China,
847 including the North Plain of China (NPC: Anhui, Shandong, Hebei, Shanxi, Tianjin,
848 Beijing), the Central of China (CC: Hunan, Henan, Hubei), the Yangtze River Delta
849 (YRD: Zhejiang, Jiangsu, Shanghai), the Northeast of China (NC: Heilongjiang,
850 Liaoning, Jilin), the Pan-Pearl River Delta (PRD: Hainan, Guangdong, Fujian,

Guangxi, Guizhou, Sichuan, Yunnan, Jiangxi), the West of China (WC: Shannxi, Chongqing, Xinjiang, Qinghai, Ningxia, Tibet, Inner Mongolia, Gansu). And the bulk-weighted burning rates that averaged from BAU, EM, and NDRC versions for the six zones were 22.3 % ± 3.1 %, 21.1 % ± 3.3 %, 28.4 % ± 6.2 %, 23.3 % ± 9.2 % 21.4 % ± 6.5 %, and 14.2 % ± 8.0 %, respectively. It was obvious that agricultural field burning was most serious in the Yangtze River Delta, especially in the Zhejiang province. The nationwide filed burning rate was 21.4 %, 16.3 %, 26.0 %, 14.9 %, and 26.8 % for BAU-I, BAU-II, EM-I, EM-II, and NDRC, respectively, which were comparable with the document values (Daize, 2000; Wei et al., 2004; Zhang et al., 2008a).

3.3.3 Agricultural open burning emissions

$PM_{2.5}$ emissions from agricultural field burnings based on BAU, EM, and NDRC versions were calculated and geographically presented in Fig. 7 (emissions of detailed individual species in SI). A similar spatial character of regional emission distribution was observed for BAU, EM, and NDRC versions, most emissions were allocated in the North Plain and the Central of China, where the primary agricultural regions locate, echoing the agricultural fire sites in Fig. S2 (SI). Although filed burning rates were higher in the Yangtze River Delta, the crop residue productions in this zone were much less, which only contributed 4.3 % of the national straw productions. Take NDRC as the basis, BAU and EM scenarios all underestimated the emissions in the Northeast of China, especially in Heilongjiang.

The temporal distributions of field burning emissions also echoed the crop residue productions and the agricultural fire sites in summer and autumn harvest. Apart from Henan and Tibet where the main crop straws were produced in summertime, more pollutants were emitted in autumn harvest period to the rest place, which has been confirmed by many studies (He et al., 2011; Wang and Zhang, 2008). And the large scale filed burning emissions in autumn exhibited great influence on the haze formation and visibility degradation in the North and East of China (Leng et al., 2014;

879 Shi et al., 2014), Huang et al. (2012a) has identified biomass burning together with
880 secondary inorganic aerosol (SIA) and dust pollution as three typical haze types in
881 Shanghai. In summertime, filed burning emissions concentrated in the North Plain, the
882 Central, and the South regions. While in autumn, the emissions became more
883 ubiquitous and serious in the Northeast of China.

884 Nationwide emission inventories and flux concentrations were graphically
885 displayed in Fig. 8 and tabular presented in Table 5. The total $PM_{2.5}$ emission from
886 agricultural field burnings was 738.36-1241.69 Gg in 2012, and rice, corn, and wheat
887 straw burnings made up 93.5% ~ 95.6% of the total emissions. The largest quantities
888 of $PM_{2.5}$ emissions were emitted from Heilongjiang, Shandong, Henan, Jilin, Jiangsu,
889 Anhui and Hebei, distinct difference in the emissions from various scenarios were
890 observed, especially for Heilongjiang province which contributed 5.5 % (55.4 Gg) of
891 $PM_{2.5}$ emissions under BAU-II scenarios, while the figure was 22.9 % (231.0 Gg)
892 under EM-I scenarios. Annual emissions of $PM_{1.0}$, OC, and EC was 661.81-1111.90,
893 318.84-533.19, and 98.06-164.97 Gg, respectively, which were comparable with the
894 precious studies (Cao et al., 2006, 2011; Wang et al., 2012). Qin and Xie (2011, 2012)
895 developed national carbonaceous aerosol emission inventories from biomass open
896 burning for multi-years with dynamic burning activity, they believed BC and OC
897 emissions followed an exponential growth from 14.03 and 57.37 Gg in 1990 to 116.58
898 and 476.77 Gg in 2009. Cao et al. (2006, 2011) calculated smoke aerosol emissions
899 from biomass burning in China for 2000 and 2007 using the same activity data from
900 BAU-I scenarios, national OC and EC emissions were reported to be 425.9 and 103.0
901 Gg in 2000, however, no evident changes were found for the emissions in 2007, which
902 were assessed to be 433.0 and 104.0 Gg. Huang et al. (2012b) estimated crop burning
903 in the fields with unified EFs and burning rate (~6.6%) for all kinds of crops across
904 China in 2006, the estimated annual agricultural fire emissions were about 270, 100,
905 and 30 Gg for $PM_{2.5}$, OC, and BC, respectively. In present work, agricultural fire
906 $PM_{2.5}$ emissions in 2012 were allocated into six zones, average contribution in
907 percentage for each zone was compared: NPC (23.1%) ≥ NC (21.6%) > PRD (18.4%)
908 ≥ CC (18.2%) > WC (9.8%) > YRD (8.8%). Furtherly, contribution for summertime

emissions was: NPC (35.5%) > CC (28.8%) ≥ PRD (21.1%) > YRD (9.1%)> WC (5.4%) > NC (0.1%), and for autumn harvest emissions: NC (27.8%) > NPC (19.6%) > PRD (17.6%) > CC (15.1%) > WC (11.1%) > YRD (8.8%). It was obviously that the North Plain experienced extensive crop fire emissions during the whole harvest periods, where $PM_{2.5}$, $PM_{1.0}$, OC, and BC emissions in 2012 were 233.6, 209.8, 102.3, and 29.4 Gg on average. Liu et al. (2015) developed emission inventories from agricultural fires in the North Plain based on MODIS fire radiative power, emission for $PM_{2.5}$, OC, and BC in 2012 was reported to be 102.3, 37.4, and 13.0 Gg, respectively. However, EFs were also treated as unified values (e.g., Crop burning EFs for $PM_{2.5}$, OC, and BC was 6.3, 2.3, and 0.8 g Kg^{-1}) in the work of Liu et al. (2015) that was cited directly from Akagi et al. (2011) without considering fuel type dependence of EFs. Zhao et al. (2012) established comprehensive anthropogenic emission inventories for Huabei Region including the North Plain, Inner Mongolia, and Liaoning province, all crop straws were assumed to be burnt in the field, resulting in much more emissions of 446 Gg OC and 160 Gg BC in 2003. A specific temporal pattern for agricultural fire emissions was observed in the Northeast of China (Heilongjiang, Liaoning, and Jilin), where the open burning were mainly occurred in autumn harvest to produce great amount of pollutants (217.5 Gg $PM_{2.5}$, 89.4 Gg OC, and 29.7 Gg EC), while emissions in the summertime can be neglected.

In 2012, 20-25 % of national emissions were released from summertime field burnings, that was 226.0 Gg $PM_{2.5}$, 205.2 Gg $PM_{1.0}$, 105.9 Gg OC, 28.4 Gg EC, 6.8 Gg WSOA, 1.0 Gg WSA, 0.1 Gg PAHs, 0.9 Gg phenols, and 2.1 Gg THM on average. The corresponded values for autumn harvest were 781.6, 697.9, 327.3, 106.0, 18.4, 4.8, 0.4, 1.9, and 6.6 Gg, respectively. Integrated smoke OC/EC was 3.7 from national summertime emission and 3.1 from autumn harvest emission, regarding to different locations, integrated OC/EC in the North Plain was 4.1 in summertime emission and 3.2 in autumn harvest, while OC/EC in the Central of China was 3.1 for both summer and autumn harvest emissions, implying temporal-spatial characters of agricultural field fires exhibit potential influence on composition of smoke emissions and its related physiochemical properties. Zhang et al. (2011) estimated particulate PAHs

939 emissions form three types of crop residues to be 0.46 Gg in 2003. Xu et al. (2006)
940 counted PAHs from all straws with the assumption that burning rates to be unit, and
941 they calculated 5-10 Gg PAHs emissions in 2003, which was ten times of our result.
942 The nationwide flux concentration of smoke $PM_{2.5}$ was 0.7-1.0 μg m^{-3} d^{-1} in
943 summer harvest and 1.4-3.5 μg m^{-3} d^{-1} in autumn harvest, while average annual flux
944 concentrations for OC and EC were 0.80 and 0.25 μg m^{-3} d^{-1}. Saikawa et al. (2009)
945 assessed the annual concentrations of OC and BC from biomass burning primary
946 emission in China using global models of chemical transport (MOZART-2) to be 1.8
947 and 0.35μg m^{-3}. The most polluted areas were Anhui, Henan, Shandong, Jiangsu,
948 Liaoning, and Hunan.

949 **3.3.4 Uncertainties of the emissions**

950 The fuzziness and uncertainties of major pollutants emissions from fuel combustion in
951 China came from the uncertainties in specific-source emission factors and effective
952 consumption of bio- or fossil fuel. Frey et al. analyzed uncertainties in emission
953 factors and emissions of air toxic pollutants and technology dependent coal-fire power
954 plants via bootstrap simulation method (Frey and Zhao, 2004; Frey and Zheng, 2002).
955 Zhao et al. estimated uncertainties in national anthropogenic pollutants emissions
956 based on Monte Carlo simulation, and they believed activity rates (e.g. fuel
957 consumption) are not the main source of emissions uncertainties at the national level
958 (Zhao et al., 2011; Zhao et al., 2012). The uncertainties in emission inventory can also
959 be estimated by comparing different emission inventories for the same region and
960 period (Ma and Van Aardenne, 2004).
961 In this study, we investigated the uncertainties of multi-pollutants emissions for
962 agricultural residue open burning using Monte Carlo Simulation. Detailed
963 methodology was referred to Qin and Xie (2011). We followed the assumption: a
964 normal distribution with coefficient of variation (CV) of 30% for the official
965 statistics (e.g., crop production and GDP economic data obtained from Statistic
966 Yearbooks, field burning rates for agricultural straw derived from NDRC report, etc.),

967 a normal distribution with 50% CV for open burning rates from literature (BAU-I and
968 BAU-II), and a uniform distribution with ± 30% deviation for the rest activity data
969 (crop-to-residue ratio, dry matter fraction, and burning efficiency). Regarding the
970 emission factors, Bond et al. (2004) assumed that most particulate EFs followed
971 lognormal distributions with CV of ± 50% for domestic EFs, and of ± 150% for EFs
972 obtained from foreign studies. Here, we applied the CV of smoke EFs as we
973 measured ones, which were chemical species and fuel type dependent. With
974 randomly selected values within the respective probability density functions (PDFs)
975 of EFs and activity data for each biomass type, Monte Carlo simulation was
976 implemented for 10,000 times, and the uncertainties in national yearly
977 multi-pollutants emissions at 95% CI were obtained for all the 5 versions. Afterwards,
978 uncertainties for the average emission inventories were assessed using the
979 propagation of uncertainty calculation that suggested by IPCC (1997) (method in SI),
980 and all the emission uncertainties were presented in percentage in Table 6. Emissions
981 for water soluble aminiums and organic acids had the vast uncertainties, due to their
982 large deviation in EFs compared with other smoke species. Besides, emissions of
983 BAU versions were more accurate than EM versions, because of more uncertainty
984 addition in the burning rates conversion using economic data for EM versions.
985 Otherwise, burning rates derived from NDRC report were assumed to have less
986 uncertainty, resulting in the least uncertainties in smoke emission assessments. On
987 average of all the 5 versions, mean, 2.5th percentile, and 97.5th percentile values for
988 smoke $PM_{2.5}$ emissions in 2012 were 1005.7, 758.3, and 1344.6 Gg, respectively. As
989 to OC emissions, mean, 2.5th percentile, and 97.5th percentile values were 432.4,
990 327.8, and 576.4 Gg, the figure for EC was 134.2, 100.9, and 187.9 Gg. Therefore,
991 the overall propagation of uncertainties for smoke $PM_{2.5}$, OC, and EC at 95% CI was
992 (-24.6%, 33.7%), (-24.4%, 33.5%), and (-24.2%, 33.3%), respectively. The
993 uncertainties for OC and EC emissions were much less than the work of Qin and Xie
994 (2011), in which emission and uncertainties were 266.7 Gg (-55.9%, 96.1%) for OC
995 and 66. 9 Gg (-53.9%, 92.6%) for EC in 2005.

3.4 Health and health-related economic impacts

3.4.1 Carcinogenic risk

Calculated CR_{SPM} for smoke $PM_{2.5}$ from wheat, corn, rice, cotton, and soybean straw burning were 5.3×10^{-6}, 3.8×10^{-6}, 2.6×10^{-6}, 0.7×10^{-6}, and 1.3×10^{-6} per μg m^{-3}, respectively. And the corresponded one in million PEL was 0.2, 0.3, 0.4, 1.4, and 0.8 μg m^{-3}. Wu et al. (2009) ever assessed unit risk of wood and fuel burning particles using metals merely, the results were 3.2×10^{-6} and 1.5×10^{-6} per μg m^{-3}, which were close to that in our study. In actual application, PEL of smoke particles should be bulk mass concentration of mixed aerosols.

It was noticeable that apart from Tibet and Qinghai, the flux concentration of smoke $PM_{2.5}$ among all the five emission versions in other regions far surpassed the PEL, especially the North Plain and the Central of China, exhibiting great potential inhalable cancer risk. For the health care, emission flux concentration should be constrained within the PEL of crop straw burning aerosol. Thus the critical filed burning rates can be derived to ensure risk aversion following Eq. (11):

$$R_k \leq \frac{10^{-6}\times S_k\times h\times T_k}{\sum_j\sum_i P_{t,k,i}\times r_i\times H_{t,k,i}\times D_i\times f_i\times EF_{i,j}\times CRF_i} \quad (11)$$

The conservative values of regional field burning rates from Eq. (11) were named as Carcinogenic Risk Control scenarios (CRC) and listed in Table S11 (SI), which would be instructive in emission control. Under CRC, national crop straw field burning rate was less than 3%, emissions of $PM_{2.5}$ were geographically presented in Fig. S4 (SI), and 146.3 Gg yr^{-1} smoke $PM_{2.5}$ should be released at largest in China, the corresponded annual flux concentration of $PM_{2.5}$ was within 0.3 μg m^{-3} d^{-1} (detailed emission inventories under CRC version see in SI).

3.4.2 Health impacts

Regional health impacts from acute exposure of agricultural residue burning aerosol were assessed using average daily flux concentrations of smoke $PM_{2.5}$, the result was tabulated in Table S12 (SI). The impacts from smoke $PM_{2.5}$ exposure were severest in

Jiangsu, Shandong, and Henan province, where annual premature mortality was over one thousand. Overall, China suffered from 7836 (95% CI: 3232, 12362) premature death, 31181 (95% CI: 21145, 40881) respiratory hospital admissions, 29520 (95% CI: 12873, 45602) cardiovascular hospital admissions, and 7267237 (95% CI: 2961487, 1130784) chronic bronchitis related to agricultural fire smoke in 2012 from Table 7. According to national health statistical reports (NHFPC, 2013), the hospital admission due to respiratory and cardiovascular disease was 5071523 in China in 2012, and smoke $PM_{2.5}$ exposure might contribute ~1.2% of the hospital admissions from this study. Saikawa et al. (2009) ever reported 70000 premature deaths in China and an additional 30000 deaths globally due to OC, EC, and sulfate exposure that were primarily emitted from biofuel combustion in China in 2000, however, the results should be overestimated not only in the exaggerated pollutant emissions but also in the iterative operations of respective species induced mortality, besides, the exposure-response coefficient β and incidence rate he applied from Pope et al. (2002) and WHO (2000) were higher than the practical values from local research (Cao et al., 2012; Chen et al., 2011; Hou et al., 2012). From Table 7, under CRC version, over 92 % mortality and morbidity can be avoided.

3.4.3 Health-related economic losses

Health-related total economic losses from straw open burning smoke $PM_{2.5}$ exposure were assessed to be 8822.4 (95% CI: 3574.4, 13034.2) million US$ on average from Table 8, accounting for 0.1% of the total GDP in 2012, and detailed regional economic losses were listed in Table S13. Economic losses from premature death contributed about 17% of total losses, and loss from chronic bronchitis dominated. Hou et al. (2012) ever estimated 106.5 billion US$ lost due to ambient PM_{10} exposure in China in 2009; even a severe haze episode ($PM_{2.5}$ be focused on) in January 2013 may cause 690 premature death and 253.8 million US$ loss in Beijing, and source-specification analysis stressed the emission from biomass burning (Yang et al., 2015; Gao et al., 2015). It was obvious that smoke $PM_{2.5}$ contributed a noticeable damage to public

health and social welfare. According to CRC version estimation, the carcinogenic risk control policy can save over 92 % of the economic loss.

4 Conclusion

Detailed chemical compositions of smoke aerosol from five major agricultural straws burning were characterized using an aerosol chamber system. And corresponded emission factors for particulate OC-EC, WSI, WSOA, WSA, PAHs, Phenols, and THM in smoke $PM_{2.5}$ and $PM_{1.0}$ were established.

Permissible exposure limits (PEL) of the smoke particles were assessed for carcinogenic risk concern based on selected hazard pollutants including PAHs and THM in smoke $PM_{2.5}$. Daily exposure concentration should be constrained within 0.2, 0.3, 0.4, 1.4, and 0.8 μg m^{-3} for wheat, corn, rice, cotton, and soybean straw, respectively.

Emission inventories of primary particulate pollutants from agricultural field burning in 2012 were estimated based on BAU-I, BAU-II, EM-I, EM-II, and NDRC scenarios, which were further allocated into different regions at summer and autumn open burning periods. The estimated total emissions were 1005.7 Gg $PM_{2.5}$ (95%CI: -24.6% , 33.7%), 901.4 Gg $PM_{1.0}$ (95%CI: -24.4%, 33.5%), 432.4 Gg OC (95%CI: -24.2%, 33.5%), 134.2 Gg EC (95%CI: -24.8%, 34.0%), 249.8 Gg WSI (95%CI: -25.4%, 34.9%), 25.1 Gg WSOA (95%CI: -33.3%, 41.4%), 5.8 Gg WSA (95%CI: -30.1%, 38.5%), 8.7 Gg THM (95%CI: -26.6%, 35.6%), 0.5 Gg PAHs (95%CI: -26.0%, 34.9%), and 2.7 Gg Phenols (95%CI: -26.1%, 35.1%), respectively. The spatial and temporal distributions of the five versions have similar characters that echo to the agricultural fires sites from satellite remote sensing. Less than 25 % of the emissions were released from summer field burnings that were mainly contributed by the North Plain and the Central of China. Flux concentrations of annual smoke $PM_{2.5}$ that were calculated using box-model method based on five versions all exceed the PEL. From assessment of health impacts and health-related economic losses due to smoke $PM_{2.5}$ short-term exposure, China suffered from 7836 (95%CI: 3232, 12362)

premature mortality and 7267237 (95% CI: 2961487, 1130784) chronic bronchitis in 2012, which led to 8822.4 (95%CI: 3574.4, 13034.2) million US$, or 0.1 % of the total GDP losses.

Percentage of open burned crop straws at post-harvest period should cut down to less than 3% to ensure risk aversion from carcinogenicity, especially the North Plain and the Northeast, where the emissions should decease at least by 94% to meet the PEL. And by applying such emission control policy, over 92% of the mortality and morbidity attributed to agricultural fire smoke $PM_{2.5}$ can be avoided in China.

Supplementary material related to this article is available online at:

Acknowledgment. This work is supported by National Natural Science Foundation of China (No. 21190053, 21177025), Cyrus Tang Foundation (No. CTF-FD2014001), Shanghai Science and Technology Commission of Shanghai Municipality (No. 13XD1400700, 12DJ1400100), Priority fields for Ph.D. Programs Foundation of Ministry of Education of China (No. 20110071130003) and Strategic Priority Research Program of the Chinese Academy of Sciences (Grant No. XDB05010200).

References:

Ackerman, A. S.: Reduction of Tropical Cloudiness by Soot, Science, 5468, 1042-1047, 2000.

Adams, P. J., Seinfeld, J. H. and Koch, D. M.: Global concentrations of tropospheric sulfate, nitrate, and ammonium aerosol simulated in a general circulation model, J. Geophys Res, D11:13791-13823, 1999.

Akagi, S. K., Yokelson, R. J., Wiedinmyer, C., Alvarado, M. J., Reid, J. S., Karl, T., Crounse, J. D. and Wennberg, P. O.: Emission factors for open and domestic biomass burning for use in atmospheric models, Atmos Chem. Phys., 9, 4039-4072, 2011.

Amdur, M. O. and Chen, L. C.: Furnace-Generated Acid Aerosols: Speciation and Pulmonary Effects, Environ. Health Persp., 79, 147-150, 1989.

Andreae, M. O. and Gelencsér, A.: Black carbon or brown carbon? The nature of light-absorbing carbonaceous aerosols, Atmos Chem. Phys., 10, 3131-3148, 2006.

Andreae, M. O. and Merlet, P.: Emission of trace gases and aerosols from biomass burning, Global Biogeochem Cy., 4, 955-966, 2001.

Andreae, M. O., Andreae, T. W., Annegarn, H., Beer, J., Cachier, H., le Canut, P., Elbert, W., Maenhaut, W., Salma, I., Wienhold, F. G., and Zenke, T. :, Airborne studies of aerosol emissions from savanna fires in southern Africa: 2. Aerosol chemical composition, J. Geophys Res., D24, 32119-32128, 1998.

Araujo, J. A., Barajas, B., Kleinman, M., Wang, X., Bennett, B. J., Gong, K. W. Navab, M., Harkema, J., Sioutas, C., Lusis, A. J., and Nel, A. E.:Ambient particulate pollutants in the ultrafine range promote early atherosclerosis and systemic oxidative stress, Circ Res., 5, 589-596, 2008.

Arey, J. and Atkinson, R.: Photochemical reactions of PAHs in the atmosphere, PAHs: An Ecotoxicological Persp., 47- 63, doi: 10.1002/0470867132.ch4, 2003.

Arora, P. and Jain, S.: Estimation of Organic and Elemental Carbon Emitted from Wood Burning in

Traditional and Improved Cookstoves Using Controlled Cooking Test, Environ. Sci. Technol., 6, 3958-3965, 2015.
Aunan, K. and Pan, X.: Exposure-response functions for health effects of ambient air pollution applicable for China-a meta-analysis, Sci. Total Environ., 329, 3-16, 2004.
Aurell, J., Gullett, B. K. and Tabor, D.: Emissions from southeastern U.S. Grasslands and pine savannas: Comparison of aerial and ground field measurements with laboratory burns, Atmos. Environ., 111, 170-178, 2015.
Bell, R. W. and Hipfner, J. C.: Airborne Hexavalent Chromium in Southwestern Ontario, J. Air Waste Manage, 8, 905-910, 1997.
Berndt, T. and Böge, O.: Formation of phenol and carbonyls from the atmospheric reaction of OH radicals with benzene, Phys. Chem. Chem. Phys., 10, 1205-1214, doi:10.1039/B514148F, 2006.
Bølling, A. K., Pagels, J., Yttri, K. E., Barregard, L., Sallsten, G., Schwarze, P. E. and Boman, C.: Health effects of residential wood smoke particles: the importance of combustion conditions and physicochemical particle properties, Part. Fibre Toxicol., 29, doi:10.1186/1743-8977-6-29, 2009.
Bond, T. C.: A technology-based global inventory of black and organic carbon emissions from combustion, J. Geophys Res., 109, D14203, doi:10.1029/2003JD003697, 2004.
Bond, T. C., Doherty, S. J., Fahey, D. W., Forster, P. M., Berntsen, T., DeAngelo, B. J. Flanner, M. G., Ghan, S., Kärcher, B., Koch, D., Kinne, S., Kondo, Y., Quinn, P. K., Sarofim, M. C., Schultz, M. G., Schulz, M., Venkataraman, C., Zhang, H., Zhang, S., Bellouin, N., Guttikunda, S. K., Hopke, P. K., Jacobson, M. Z., Kaiser, J. W., Klimont, Z., Lohmann, U., Schwarz, J., PShindell, D., Storelvmo, T., Warren, S. G., and Zender, C. S.: Bounding the role of black carbon in the climate system: A scientific assessment, J. Geophys Res: Atmos, 11, 5380-5552, 2013.
Bruce, R. M., Santodonato, J. and Neal, M. W.: Summary Review of the Health Effects Associated With Phenol, Toxicol Ind. Health, 4, 535-568, 1987.
Buha, J., Mueller, N., Nowack, B., Ulrich, A., Losert, S. and Wang, J.: Physical and Chemical Characterization of Fly Ashes from Swiss Waste Incineration Plants and Determination of the Ash Fraction in the Nanometer Range, Environ. Sci. Technol., 9, 4765-4773, 2014.
Burkart, K., Nehls, I., Win, T. and Endlicher, W.: The carcinogenic risk and variability of particulate-bound polycyclic aromatic hydrocarbons with consideration of meteorological conditions, Air Quality, Atmos. Health, 1, 27-38, 2013.
Bzdek, B. R., Ridge, D. P. and Johnston, M. V.: Amine reactivity with charged sulfuric acid clusters, Atmos. Chem. Phys., 16, 8735-8743, 2011.
Bzdek, B. R., Ridge, D. P. and Johnston, M. V., Amine exchange into ammonium bisulfate and ammonium nitrate nuclei, Atmos Chem Phys, 8:3495-3503, 2010.
Cao, G., Zhang, X. and Zheng, F.: Inventory of black carbon and organic carbon emissions from China, Atmos. Environ., 34, 6516-6527, 2006.
Cao, G., Zhang, X., Gong, S., An, X. and Wang, Y.: Emission inventories of primary particles and pollutant gases for China, Chinese Sci. Bull, 8, 781-788, 2011.
Cao, G., Zhang, X., Wang, D. and Zheng, F.: Inventory of Emissions of Pollutants from Open Burning Crop Residues, J. Agro-Environ. Sci., 4, 800-804, 2005.
Cao, J., Xu, H., Xu, Q., Chen, B. and Kan, H.: Fine particulate matter constituents and cardiopulmonary mortality in a heavily polluted Chinese city, Environ. Health Persp., 3, 373, 2012.
Carlton, A. G., Turpin, B. J., Lim, H., Altieri, K. E. and Seitzinger, S.: Link between isoprene and secondary organic aerosol (SOA): Pyruvic acid oxidation yields low volatility organic acids in clouds,

Geophys. Res. Lett., Lo6822, doi:10.1029/2005GL025374, 2006.
Cermak, J. and Knutti, R.: Beijing Olympics as an aerosol field experiment, Geophys. Res. Lett., 36, L10806, doi:10.1029/2009GL038572, 2009.
Chakrabarty, R. K., Moosmüller, H., Chen, L. W. A., Lewis, K., Arnott, W. P., Mazzoleni, C., Dubey, M. K., Wold, C. E., Hao, W. M., and Kreidenweis, S. M.: Brown carbon in tar balls from smoldering biomass combustion, Atmos. Chem. Phys., 13, 6363-6370, 2010.
Chan, M. N., Choi, M. Y., Ng, N. L. and Chan, C. K.: Hygroscopicity of Water-Soluble Organic Compounds in Atmospheric Aerosols: Amino Acids and Biomass Burning Derived Organic Species, Environ. Sci. Technol., 6, 1555-1562, 2005.
Chen, H., Hu, D., Wang, L., Mellouki, A. and Chen, J.: Modification in light absorption cross section of laboratory-generated black carbon-brown carbon particles upon surface reaction and hydration, Atmos. Environ., 116, 253-261, 2015.
Chen, R., Li, Y., Ma, Y., Pan, G., Zeng, G., Xu, X., Chen, B. and Kan, H.: Coarse particles and mortality in three Chinese cities: The China Air Pollution and Health Effects Study (CAPES), Sci. Total Environ., 23, 4934-4938, 2011.
Cheng, Y., Ho, K. F., Lee, S. C. and Law, S. W.: Seasonal and diurnal variations of $PM_{1.0}$, $PM_{2.5}$ and PM_{10} in the roadside environment of Hong Kong, China Particuology, 06:312-315, 2006.
China Ministry of Health (CMH): China statistical yearbook of public health, Peking Union Medical College Press, 172–189, 2009. (*In Chinese*)
Christopher, S. A., Chou, J., Zhang, J., Li, X., Berendes, T. and Welch, R. M.: Shortwave direct radiative forcing of biomass burning aerosols estimated using VIRS and CERES data, Geophys. Res. Lett., 15, 2197-2200, 2000.
Clarke, A., McNaughton, C., Kapustin, V., Shinozuka, Y., Howell, S., Dibb, J., Zhou, J., Anderson, B., Brekhovskikh, V., Turner, H. and Pinkerton, M.: Biomass burning and pollution aerosol over North America: Organic components and their influence on spectral optical properties and humidification response, J. Geophys. Res., D12, doi:10.1029/2006JD007777, 2007.
Cwiertny, D. M., Baltrusaitis, J., Hunter, G. J., Laskin, A., Scherer, M. M. and Grassian, V. H.: Characterization and acid-mobilization study of iron-containing mineral dust source materials, J. Geophys. Res.: Atmos., D5, doi:10.1029/2007JD009332, 2008.
Daize, H.: The Utilizing Status and Prospects of the Crop Straw Resources in China, Resource Development & Market:12, 2000.
Davidson, C. I., Phalen, R. F. and Solomon, P. A.: Airborne Particulate Matter and Human Health: A Review, Aerosol Sci. Tech., 8, 737-749, 2005.
Delfino, R. J., Sioutas, C. and Malik, S.: Potential role of ultrafine particles in associations between airborne particle mass and cardiovascular health, Environ. Health Perspect., 8, 934-946, 2005.
Dentener, F. J., Carmichael, G. R., Zhang, Y., Lelieveld, J. and Crutzen, P. J.: Role of mineral aerosol as a reactive surface in the global troposphere, J. Geophys. Res., D17, 22869-22889, doi: 10.1029/96JD01818, 1996.
Dhammapala, R., Claiborn, C., Corkill, J. and Gullett, B.: Particulate emissions from wheat and Kentucky bluegrass stubble burning in eastern Washington and northern Idaho, Atmos. Environ., 6, 1007-1015, 2006.
Dhammapala, R., Claiborn, C., Jimenez, J., Corkill, J., Gullett, B., Simpson, C. and Paulsen, M.: Emission factors of PAHs, methoxyphenols, levoglucosan, elemental carbon and organic carbon from simulated wheat and Kentucky bluegrass stubble burns, Atmos. Environ., 12, 2660-2669, 2007a.

1204 Dhammapala, R., Claiborn, C., Simpson, C. and Jimenez, J.: Emission factors from wheat and Kentucky
1205 bluegrass stubble burning: Comparison of field and simulated burn experiments, Atmos. Environ., 7,
1206 1512-1520, 2007b.
1207 Dusek, U., Frank, G. P., Hildebrandt, L., Curtius, J., Schneider, J., Walter, S., Chand, D., Drewnick, F.,
1208 Hings, S., Jung, D.: Size matters more than chemistry for cloud-nucleating ability of aerosol particles,
1209 Science, 5778, 1375-1378, 2006.
1210 Echalar, F., Gaudichet, A., Cachier, H. and Artaxo, P.: Aerosol emissions by tropical forest and savanna
1211 biomass burning: Characteristic trace elements and fluxes, Geophys. Res. Lett., 22, 3039-3042,
1212 doi:10.1029/95GL03170, 1995.
1213 Engelhart, G. J., Hennigan, C. J., Miracolo, M. A., Robinson, A. L. and Pandis, S. N.: Cloud
1214 condensation nuclei activity of fresh primary and aged biomass burning aerosol, Atmos. Chem. Phys., 15,
1215 7285-7293, doi:10.5194/acp- 12- 7285- 2012, 2012.
1216 Falkovich, A. H., E., R. G., G., S., Y., R., Maenhaut, W. and Artaxo, P.: Low molecular weight organic
1217 acids in aerosol particles from Rondônia, Brazil, during the biomass-burning, transition and wet periods,
1218 Atmos. Chem. Phys., 5, 781-797, doi:10.5194/acp-5-781-2005, 2005.
1219 Frey, H. C. and Zhao, Y.: Quantification of Variability and Uncertainty for Air Toxic Emission
1220 Inventories with Censored Emission Factor Data, Environ. Sci. Technol., 22, 6094-6100, 2004.
1221 Frey, H. and Zheng, J.: Quantification of variability and uncertainty in air pollutant emission inventories:
1222 method and case study for utility NOx emissions, J. Air Waste Manag. Assoc., 9, 1083-1095, 2002.
1223 Fu, H., Zhang, M., Li, W., Chen, J., Wang, L., Quan, X. and Wang, W.: Morphology, composition and
1224 mixing state of individual carbonaceous aerosol in urban Shanghai, Atmos. Chem. Phys., 2, 693-707,
1225 2012.
1226 Galarneau, E.: Source specificity and atmospheric processing of airborne PAHs: Implications for source
1227 apportionment, Atmos. Environ., 35, 8139-8149, 2008.
1228 Gao, M., Guttikunda, S. K., Carmichael, G. R., Wang, Y., Liu, Z., Stanier, C. O., Saide, P. E. and Yu, M.:
1229 Health impacts and economic losses assessment of the 2013 severe haze event in Beijing area, Sci. Total
1230 Environ., 511, 553-561, 2015.
1231 Gao, S., Hegg, D. A., Hobbs, P. V., Kirchstetter, T. W., Magi, B. I. and Sadilek, M.: Water-soluble
1232 organic components in aerosols associated with savanna fires in southern Africa: Identification,
1233 evolution, and distribution, J. Geophys.l Res.: Atmos., D13, doi:10.1029/2002JD002324, 2003.
1234 Ge, X., Wexler, A. S. and Clegg, S. L.: Atmospheric amines-Part I. A review, Atmos. Environ., 3,
1235 524-546, 2011.
1236 Ghorai, S., Wang, B., Tivanski, A. and Laskin, A.: Hygroscopic Properties of Internally Mixed Particles
1237 Composed of NaCl and Water-Soluble Organic Acids, Environ. Sci. Technol., doi: 10.1021/es404727u,
1238 2014.
1239 Giordano, M., Espinoza, C. and Asa-Awuku, A.: Experimentally measured morphology of biomass
1240 burning aerosol and its impacts on CCN ability, Atmos. Chem. Phys., 4, 1807-1821, 2015.
1241 Grieshop, A. P., Logue, J. M., Donahue, N. M. and Robinson, A. L.: Laboratory investigation of
1242 photochemical oxidation of organic aerosol from wood fires 1: measurement and simulation of organic
1243 aerosol evolution, Atmos. Chem. Phys., 4, 1263-1277, 2009.
1244 Guttikunda, S. K. and Kopakka, R. V.: Source emissions and health impacts of urban air pollution in
1245 Hyderabad, India, Air Quality, Atmos. & Health, 2, 195-207, 2014.
1246 Han, Y. M., Chen, L., Huang, R., Chow, J. C., Watson, J. G., Ni, H. Y., Liu, S. X., Fung, K. K., Shen, Z.
1247 X. and Wei, C.: Carbonaceous aerosols in megacity Xi'an, China: Implications of thermal/optical

protocols comparison, Atmos. Environ., 132, 58-68, 2016.
Han, Y. M., Lee, S. C., Cao, J. J., Ho, K. F. and An, Z. S.: Spatial distribution and seasonal variation of char-EC and soot-EC in the atmosphere over China, Atmos. Environ., 38, 6066-6073, 2009.
Han, Y., Cao, J., Chow, J. C., Watson, J. G., An, Z., Jin, Z., Fung, K. and Liu, S.: Evaluation of the thermal/optical reflectance method for discrimination between char- and soot-EC, Chemosphere, 4, 569-574, 2007.
Hayashi, K., Ono, K., Kajiura, M., Sudo, S., Yonemura, S., Fushimi, A., Saitoh, K., Fujitani, Y. and Tanabe, K.: Trace gas and particle emissions from open burning of three cereal crop residues: Increase in residue moistness enhances emissions of carbon monoxide, methane, and particulate organic carbon, Atmos. Environ., 95, 36-44, 2014.
Hays, M. D., Fine, P. M., Geron, C. D., Kleeman, M. J. and Gullett, B. K.: Open burning of agricultural biomass: physical and chemical properties of particle-phase emissions, Atmos. Environ., 36, 6747-6764, 2005.
He, K., Zhao, Q., Ma, Y., Duan, F. and Yang, F.: Spatial and seasonal variability of $PM_{2.5}$ acidity at two Chinese megacities: insights into the formation of secondary inorganic aerosols, Atmos. Chem. Phys. Dis., 25557-25603, doi:10.5194/acpd- 11- 25557- 2011, 2011a.
He, M., Zheng, J., Yin, S. and Zhang, Y.: Trends, temporal and spatial characteristics, and uncertainties in biomass burning emissions in the Pearl River Delta, China, Atmos. Environ., 24, 4051-4059, 2011b.
Ho, K. F., Ho, S. S. H., Huang, R., Liu, S. X., Cao, J., Zhang, T., Chuang, H., Chan, C. S., Hu, D. and Tian, L.: Characteristics of water-soluble organic nitrogen in fine particulate matter in the continental area of China, Atmos. Environ., 106, 252-261, 2015.
Hou, Q., An, X., Wang, Y., Tao, Y. and Sun, Z.: An assessment of China's PM_{10}-related health economic losses in 2009, Sci. Total. Environ., 61-65, 2012.
Hu, Y., Lin, J., Zhang, S., Kong, L., Fu, H. and Chen, J.: Identification of the typical metal particles among haze, fog, and clear episodes in the Beijing atmosphere, Sci. Total Environ., 369-380, 2015.
Huang, K., Zhuang, G., Lin, Y., Fu, J. S., Wang, Q., Liu, T., Zhang, R., Jiang, Y., Deng, C. and Fu, Q.: Typical types and formation mechanisms of haze in an Eastern Asia megacity, Shanghai, Atmos. Chem. Phys., 2012a.
Huang, K., Zhuang, G., Lin, Y., Wang, Q., Fu, J. S., Fu, Q., Liu, T. and Deng, C.: How to improve the air quality over megacities in China: pollution characterization and source analysis in Shanghai before, during, and after the 2010 World Expo, Atmos. Chem. Phys., 12, 5927-5942, 2013.
Huang, R., Zhang, Y., Bozzetti, C., Ho, K., Cao, J., Han, Y., Daellenbach, K. R.,Slowik, J. G., Platt, S. M., Canonaco, F., Zotter, P., Wolf, R., Pieber, S., Bruns, E., Crippa, M., Ciarelli, G., Piazzalunga, A., Schnelle-Kreis, J., Zimmermann, R., An, Z., Szidat, S., Baltensperger, U., Haddad, I. and Prevot, A.: High secondary aerosol contribution to particulate pollution during haze events in China, Nature, 2014.
Huang, S., Hsu, M. and Chan, C.: Effects of submicrometer particle compositions on cytokine production and lipid peroxidation of human bronchial epithelial cells., Environ. Health Persp., 4, 478, 2003.
Huang, X., Li, M., Li, J. and Song, Y.: A high-resolution emission inventory of crop burning in fields in China based on MODIS Thermal Anomalies/Fire products, Atmos. Environ., 9-15, 2012b.
Huo, J., Lu, X., Wang, X., Chen, H., Ye, X., Gao, S., Gross, D. S., Chen, J. and Yang, X.: Online single particle analysis of chemical composition and mixing state of crop straw burning particles: from laboratory study to field measurement, Front Env. Sci. Eng., 2, 244-252, 2016.
IBRD and SEPA, Cost of pollution in China: economic estimates of physical damages, 2007, pp. 1-128.

IPCC, Greenhouse Gas Inventory Reference Manual: Revised 2006 IPCC Guidelines for National Greenhouse Gas Inventories. IPCC/OECD/IES, UK. Meteorological Office, Bracknell, UK., 2007.

IPCC, Quantifying Uncertainties in Practice, Chapter 6: Good Practice Guidance and Uncertainty Management in National Greenhouse Gas Inventories: In: IES, IPCC, OECD, et al. Bracknell, UK, 1997.

Janssen, N. A. H., Hoek, G., Simic-Lawson, M., Fischer, P., van Bree, L., Ten Brink, H., Keuken, M., Atkinson, R., Anderson, H., Brunekreef, B. and Cassee, F.: Black Carbon as an Additional Indicator of the Adverse Health Effects of Airborne Particles Compared with PM_{10} and $PM_{2.5}$, Environ. Health Persp., 12, 1691-1699, 2011.

Jayarathne, T., Stockwell, C. E., Yokelson, R. J., Nakao, S. and Stone, E. A.: Emissions of fine particle fluoride from biomass burning, Environ. Sci. Technol., 21, 12636-12644, 2014.

Jenkins, B. M., Jones, A. D., Turn, S. Q. and Williams, R. B.: Emission factors for polycyclic aromatic hydrocarbons from biomass burning, Environ. Sci. Technol., 8, 2462-2469, 1996.

Jickells, T. D., An, Z. S., Andersen, K. K., Baker, A. R., Bergametti, G., J, N. B. J., Duce, R. A., Hunter, H., Mahowald, N. and Prospero, A.: Global Iron Connections Between Desert Dust, Ocean Biogeochemistry, and Climate, Science, 308, 67-71, 2005.

Kennedy, I. M.: The health effects of combustion-generated aerosols, P. Combust Inst, 2, 2757-2770, 2007.

Kim, K., Jahan, S. A., Kabir, E. and Brown, R. J.: A review of airborne polycyclic aromatic hydrocarbons (PAHs) and their human health effects, Environ Int., 71-80, 2013.

Kong, L., Yang, Y., Zhang, S., Zhao, X., Du, H., Fu, H., Zhang, S., Cheng, T., Yang, X. and Chen, J.: Observations of linear dependence between sulfate and nitrate in atmospheric particles, J. Geophys. Res.: Atmos., 1, 341-361, doi:10.1002/2013JD020222, 2014.

Koopmans, A. and Koppejan, J.: Agricultural and forest residue-generation, utilization and availability, Modern Applications of Biomass Energy, 1997.

Korenaga, T., Liu, X. and Huang, Z.: The influence of moisture content on polycyclic aromatic hydrocarbons emission during rice straw burning, Chemosphere-Global Change Science, 1, 117-122, 2001

Kundu, S., Kawamura, K., Andreae, T. W., Hoffer, A. and Andreae, M. O.: Molecular distributions of dicarboxylic acids, ketocarboxylic acids and α-dicarbonyls in biomass burning aerosols: implications for photochemical production and degradation in smoke layers, Atmos. Chem. Phys., 5, 2209-2225, 2010.

Laskin, A., Laskin, J. and Nizkorodov, S. A.: Chemistry of atmospheric brown carbon, Chem. Rev., 10, 4335-4382, 2015.

Lavanchy, V. M. H., G Ggeler, H. W., Nyeki, S. and Baltensperger, U.: Elemental carbon (EC) and black carbon (BC) measurements with a thermal method and an aethalometer at the high-alpine research station Jungfraujoch, Atmos. Environ., 17, 2759-2769, 1999.

Lee, A. K. Y., Willis, M. D., Healy, R. M., Wang, J. M., Jeong, C. H., Wenger, J. C., Evans, G. J. and Abbatt, J.: Single particle characterization of biomass burning organic aerosol (BBOA): evidence for non-uniform mixing of high molecular weight organics and potassium, Atmos. Chem. Phys. Dis., 22, 32157-32183, 2015.

Lee, D. and Wexler, A. S.: Atmospheric amines-Part III: Photochemistry and toxicity, Atmos. Environ., 95-103, 2013.

Lee, R. G. M., Coleman, P., Jones, J. L., Jones, K. C. and Lohmann, R.: Emission Factors and Importance of PCDD/Fs, PCBs, PCNs, PAHs and PM_{10} from the Domestic Burning of Coal and Wood in the U.K., Environ. Sci. Technol., 6, 1436-1447, 2005.

Leng, C., Zhang, Q., Zhang, D., Xu, C., Cheng, T., Zhang, R., Tao, J., Chen, J., Zha, S. and Zhang, Y.: Variations of cloud condensation nuclei (CCN) and aerosol activity during fog-haze episode: a case study from Shanghai, Atmos. Chem. Phys., 22, 12499-12512, doi:10.5194/acp-14-12499-2014, 2014.
Lewis, K. A., Arnott, W. P., Moosmuller, H., Chakrabarty, R. K., Carrico, C. M., Kreidenweis, S. M., Day, D. E., Malm, W., Laskin, A., Jimenez, J., Ulbrich, I., Huffman, J., Onasch, T., Trimborn, A., Liu, L. and Mishchenko, M.: Reduction in biomass burning aerosol light absorption upon humidification: roles of inorganically-induced hygroscopicity, particle collapse, and photoacoustic heat and mass transfer, Atmos. Chem. Phys., 9, 8949-8966, 2009.
Levin, E. J. T., McMeeking, G. R., Carrico, C. M., Mack, L. E., Kreidenweis, S. M., Wold, C. E., Moosmüller, H., Arnott, W., Hao, W., Collett, J. and Malm, W.: Biomass burning smoke aerosol properties measured during Fire Laboratory at Missoula Experiments (FLAME), J. Geophys Res, D18210, doi:10.1029/2009JD013601, 2010.
Li, C., Ma, Z., Chen, J., Wang, X., Ye, X., Wang, L., Yang, X., Kan, H., Donaldson, D. and Mellouki, A.: Evolution of biomass burning smoke particles in the dark, Atmos. Environ., 120, 244-252, 2015.
Li, C., Hu, Y., Chen, J., Ma, Z., Ye, X., Yang, X., Wang, L., Wang, X. and Mellouki, A.: Physiochemical properties of carbonaceous aerosol from agricultural residue burning: Density, volatility, and hygroscopicity, Atmos. Environ., 2016.
Li, J., Pósfai, M., Hobbs, P. V. and Buseck, P. R.: Individual aerosol particles from biomass burning in southern Africa: 2, Compositions and aging of inorganic particles, J. Geophys. Res.: Atmos., (1984-2012), D13, doi:10.1029/2002JD002310, 2003.
Li, X., Wang, S., Duan, L., Hao, J., Li, C., Chen, Y. and Yang, L.: Particulate and trace gas emissions from open burning of wheat straw and corn stover in China, Environ. Sci. Techno., 17, 6052-6058, 2007.
Lima, A. L. C., Farrington, J. W. and Reddy, C. M.: Combustion-Derived Polycyclic Aromatic Hydrocarbons in the Environment-A Review, Environ. Forensics., 2, 109-131, 2005.
Lin, J., Nielsen, C. P., Zhao, Y., Lei, Y., Liu, Y. and McElroy, M. B.: Recent changes in particulate air pollution over China observed from space and the ground: effectiveness of emission control, Environ. Sci. Technol., 20, 7771-7776, 2010.
Lin, P., Aiona, P. K., Li, Y., Shiraiwa, M., Laskin, J., Nizkorodov, S. A. and Laskin, A.: Molecular Characterization of Brown Carbon in Biomass Burning Aerosol Particles, Environ. Sci. Technol., 21, 11815-11824, 2016.
Liu, M., Song, Y., Yao, H., Kang, Y., Li, M., Huang, X. and Hu, M.: Estimating emissions from agricultural fires in the North China Plain based on MODIS fire radiative power, Atmos. Environ., 326-334, 2015.
Liu, Q. and Bei, Y.: Impacts of crystal metal on secondary aliphatic amine aerosol formation during dust storm episodes in Beijing, Atmos. Environ., 227-234, 2016.
Lobert, J. M., Scharffe, D. H., Hao, W. M. and Crutzen, P. J.: Importance of biomass burning in the atmospheric budgets of nitrogen-containing gases, 6284, 552-554, 1990.
Lu, Z., Zhang, Q. and Streets, D. G.: Sulfur dioxide and primary carbonaceous aerosol emissions in China and India, 1996-2010, Atmos. Chem. Phys., 11, 9839-9864, doi:10.5194/acp-11-9839-2011, 2011.
Ma, J. and Van Aardenne, J. A.: Impact of different emission inventories on simulated tropospheric ozone over China: a regional chemical transport model evaluation, Atmos. Chem. Phys., 4, 877-887, 2004.
May, A. A., McMeeking, G. R., Lee, T., Taylor, J. W., Craven, J. S., Burling, I., Sullivan, A. P., Akagi, S., Collett, J., Flynn, M., Coe, H., Urbanski, S., Seinfeld, J., Yokelson, R. and Kreidenweis, S.: Aerosol

emissions from prescribed fires in the United States: A synthesis of laboratory and aircraft measurements, J. Geophys. Res.: Atmos., 20, 11826-11849, doi:10.1002/2014JD021848, 2014.
Meskhidze, N.: Dust and pollution: A recipe for enhanced ocean fertilization? J. Geophys. Res, D3, doi:10.1029/2004JD005082, 2005.
Mikhailov, E. F., Vlasenko, S. S., Podgorny, I. A., Ramanathan, V. and Corrigan, C. E.: Optical properties of soot-water drop agglomerates: An experimental study, J. Geophys. Re., 111, D07209, doi:10.1029/2005JD006389, 2006.
Moreno, T., Karanasiou, A., Amato, F., Lucarelli, F., Nava, S., Calzolai, G., Chiari, M., Coz, E., Artinano, B., Lumbreras, J., Borge, R., Boldo, R., Linares, C., Alastursy, A., Querol, X. and Gibbons, X.: Daily and hourly sourcing of metallic and mineral dust in urban air contaminated by traffic and coal-burning emissions, Atmos. Environ., 68, 33-44, 2013.
NBSC, China Statistical Yearbook 2013: China Statistics Press Beijing, China, 2013.
NHFPC, National Health and Family Planning Yearbook: Peking Union Medical College Press, 2013, p. 415.
Oanh, N. T. K., Ly, B. T., Tipayarom, D., Manandhar, B. R., Prapat, P., Simpson, C. D. and Liu, L. S.: Characterization of particulate matter emission from open burning of rice straw, Atmos. Environ., 2, 493-502, 2011.
Ostro, B. and Chestnut, L.: Assessing the health benefits of reducing particulate matter air pollution in the United States, Environ. Res., 2, 94-106, 1998.
Pope III, C. A., Burnett, R. T., Thun, M. J., Calle, E. E., Krewski, D., Ito, K. and Thurston, G. D.: Lung cancer, cardiopulmonary mortality, and long-term exposure to fine particulate air pollution, Jama, 9, 1132-1141, 2002.
Pope, C. A., Burnett, R. T., Thurston, G. D., Thun, M. J., Calle, E. E., Krewski, D. and Godleski, J. J.: Cardiovascular mortality and long-term exposure to particulate air pollution epidemiological evidence of general pathophysiological pathways of disease, Circulation, 1, 71-77, 2004.
Pósfai, M.: Atmospheric tar balls: Particles from biomass and biofuel burning, J. Geophys. Res., 109, D06213, doi:10.1029/2003JD004169, 2004.
Qin, Y. and Xie, S. D.: Spatial and temporal variation of anthropogenic black carbon emissions in China for the period 1980-2009, Atmos. Chem. Phys., 11, 4825-4841, 2012.
Qin, Y. and Xie, S. D.: Historical estimation of carbonaceous aerosol emissions from biomass open burning in China for the period 1990-2005, Environ Pollut., 12, 3316-3323, 2011.
Qiu, C. and Zhang, R.: Physiochemical Properties of Alkylaminium Sulfates: Hygroscopicity, Thermostability, and Density, Environ. Sci. Technol., 8, 4474-4480, 2012.
Qiu, C., Wang, L., Lal, V., Khalizov, A. F. and Zhang, R.: Heterogeneous Reactions of Alkylamines with Ammonium Sulfate and Ammonium Bisulfate, Environ. Sci. Technol., 11, 4748-4755, 2011.
Ram, K., Sarin, M. M. and Tripathi, S. N.: Temporal Trends in Atmospheric $PM_{2.5}$, PM_{10}, Elemental Carbon, Organic Carbon, Water-Soluble Organic Carbon, and Optical Properties: Impact of Biomass Burning Emissions in The Indo-Gangetic Plain, Environ. Sci. Technol., 2, 686-695, 2011.
Ram, K. and Sarin, M. M.: Day-night variability of EC, OC, WSOC and inorganic ions in urban environment of Indo-Gangetic Plain: implications to secondary aerosol formation, Atmos. Environ., 2, 460-468, 2011.
Reddy, M. S. and Venkataraman, C.: Atmospheric optical and radiative effects of anthropogenic aerosol constituents from India, Atmos. Environ., 34, 4511-4523, 2000.
Reid, J. S., Eck, T. F., Christopher, S. A., Koppmann, R., Dubovik, O., Eleuterio, D. P., Holben, B. N.,

Reid, E. A. and Zhang, J.: A review of biomass burning emissions part III: intensive optical properties of biomass burning particles, Atmos. Chem. Phys., 5, 827-849, 2005a.
Reid, J. S., Koppmann, R., Eck, T. F. and Eleuterio, D. P.: A review of biomass burning emissions part II: intensive physical properties of biomass burning particles, Atmos. Chem. Phys., 3, 799-825, 2005b.
Richter, H. and J, H.: Formation of polycyclic aromatic hydrocarbons and their growth to soot-a review of chemical reaction pathways, Prog Energ Combust, 4, 565-608, 2000.
Ripoll, A., Minguillón, M. C., Pey, J., Pérez, N., Querol, X. and Alastuey, A.: Joint analysis of continental and regional background environments in the western Mediterranean: PM_1 and PM_{10} concentrations and composition, Atmos. Chem. Phys., 2, 1129-1145, doi:10.5194/acp-15-1129-2015, 2015.
Roemer, W. H. and van Wijnen, J. H.: Differences among Black Smoke, PM_{10}, and $PM_{1.0}$ Levels at Urban Measurement Sites, Environ. Health Persp., 2, 151-153, 2001.
Rose, D., Gunthe, S. S., Su, H., Garland, R. M., Yang, H., Berghof, M., Cheng, Y. F., Wehner, B., Achtert, P., Nowak, A., Wiedensohler, A., Takegawa, N., Kondo, Y., Hu, M., Zhang, Y., Andreae, M. and Poschl, U.: Cloud condensation nuclei in polluted air and biomass burning smoke near the mega-city Guangzhou, China-Part 2: Size-resolved aerosol chemical composition, diurnal cycles, and externally mixed weakly CCN-active soot particles, Atmos. Chem. Phys., 6, 2817-2836, doi:10.5194/acp-11-2817-2011, 2011.
Rosenfeld, D.: Atmosphere: Aerosols, Clouds, and Climate, Science, 5778, 1323-1324, 2006.
Safai, P. D., Raju, M. P., Budhavant, K. B., Rao, P. and Devara, P.: Long term studies on characteristics of black carbon aerosols over a tropical urban station Pune, India, Atmos. Res., 173-184, 2013.
Saffari, A., Daher, N., Samara, C., Voutsa, D., Kouras, A., Manoli, E., Karagkiozidou, O., Vlachokostas, C., Moussiopoulos, N., Shafer, M., Schauer, J. and Sioutas, C.: Increased Biomass Burning Due to the Economic Crisis in Greece and Its Adverse Impact on Wintertime Air Quality in Thessaloniki, Environ. Sci. Technol., 23, 13313-13320, 2013.
Saikawa, E., Naik, V., Horowitz, L. W., Liu, J. and Mauzerall, D. L.: Present and potential future contributions of sulfate, black and organic carbon aerosols from China to global air quality, premature mortality and radiative forcing, Atmos. Environ., 17, 2814-2822, 2009.
Samy, S. and Hays, M. D.: Quantitative LC-MS for water-soluble heterocyclic amines in fine aerosols ($PM_{2.5}$) at Duke Forest, USA, Atmos. Environ., 77-80, 2013.
Santodonato, J.: Review of the estrogenic and antiestrogenic activity of polycyclic aromatic hydrocarbons: relationship to carcinogenicity, Chemosphere, 4, 835-848, 1997.
Schade, G. W. and Crutzen, P. J.: Emission of aliphatic amines from animal husbandry and their reactions: Potential source of N_2O and HCN, J. Atmos. Chem., 3, 319-346, 1995.
Schauer, J. J., Kleeman, M. J., Cass, G. R. and Simoneit, B. R. T.: Measurement of Emissions from Air Pollution Sources. 3. C1−C29 Organic Compounds from Fireplace Combustion of Wood, Environ. Sci. Technol., 9, 1716-1728, 2001.
Schlesinger, R. B.: Comparative deposition of inhaled aerosols in experimental animals and humans: a review, Journal of Toxicology and Environmental Health, Part A Current Issues, 2, 197-214, 1985.
Seinfeld, J. H. and Pandis, S. N.: Atmospheric chemistry and physics: from air pollution to climate change: John Wiley & Sons, 2012.
Sen, A., Mandal, T. K., Sharma, S. K., Saxena, M., Gupta, N. C., Gautam, R., Gupta, A., Gill, T., Rani, S., Saud, T., Singh, D. and Gadi, R.: Chemical properties of emission from biomass fuels used in the rural sector of the western region of India, Atmos. Environ., 411-424, 2014.

Shi, Y., Chen, J., Hu, D., Wang, L., Yang, X. and Wang, X.: Airborne submicron particulate (PM_1) pollution in Shanghai, China: Chemical variability, formation/dissociation of associated semi-volatile components and the impacts on visibility, Sci. Total. Environ., 199-206, 2014.

Shindell, D., Kuylenstierna, J. C. I., Vignati, E., van Dingenen, R., Amann, M., Klimont, Z., Anenberg, S. C., Muller, N., Janssens-Maenhout, G., Raes, F., Schwartz, J., Faluvegi, G., Pozzoli, L., Kupiainen, K., Hoglund-Isaksson, L., Emberson, L., Streets, D., Ramanathan, V., Hicks, K., Oanh, N., Milly, G., Williams, M., Demkin, V. and Fowler, D.: Simultaneously Mitigating Near-Term Climate Change and Improving Human Health and Food Security, Science, 6065, 183-189, 2012.

Simcik, M. F., Eisenreich, S. J. and Lioy, P. J.: Source apportionment and source/sink relationships of PAHs in the coastal atmosphere of Chicago and Lake Michigan, Atmos. Environ., 30, 5071-5079, 1999.

Simoneit, B. R. T., Rushdi, A. I., Bin Abas, M. R. and Didyk, B. M.: Alkyl Amides and Nitriles as Novel Tracers for Biomass Burning, Environ. Sci. Technol, 1, 16-21, 2003.

Streets, D. G.: Dissecting future aerosol emissions: Warming tendencies and mitigation opportunities, Climatic Change, 3-4, 313-330, 2007.

Sun, J., Peng, H., Chen, J., Wang, X., Wei, M., Li, W., Yang, L., Zhang, L., Wang, W. and Mellouki, A.: An estimation of CO_2 emission via agricultural crop residue open field burning in China from 1996 to 2013, J. Clean Prod, 2625-2631, 2016.

Takegawa, N., Miyakawa, T., Kawamura, K. and Kondo, Y.: Contribution of Selected Dicarboxylic and ω-Oxocarboxylic Acids in Ambient Aerosol to the m/z 44 Signal of an Aerodyne Aerosol Mass Spectrometer, Aerosol Sci. Tech., 41, 418-437, 2007.

Tao, Y., Ye, X., Jiang, S., Yang, X., Chen, J., Xie, Y. and Wang, R.: Effects of amines on particle growth observed in new particle formation events, J. Geophys. Res.: Atmos., 121, 324-335, doi:10.1002/2015JD024245, 2016.

Tian, D., Hu, Y., Wang, Y., Boylan, J. W., Zheng, M. and Russell, A. G.: Assessment of Biomass Burning Emissions and Their Impacts on Urban and Regional $PM_{2.5}$: A Georgia Case Study, Environ Sci. Technol., 2, 299-305, 2008.

Tóth, A., Hoffer, A., Nyirő-Kósa, I., Pósfai, M. and Gelencsér, A.: Atmospheric tar balls: aged primary droplets from biomass burning? Atmos. Chem. Phys. Dis., 12, 33089-33104, doi:10.5194/acp-14-6669-2014, 2013.

Tsai, P. J., Shieh, H. Y., Lee, W. J. and Lai, S. O.: Health-risk assessment for workers exposed to polycyclic aromatic hydrocarbons (PAHs) in a carbon black manufacturing industry, Sci. Total. Environ., 1-3, 137-150, 2001.

Urban, R. C., Alves, C. A., Allen, A. G., Cardoso, A. A. and Campos, M.: Organic aerosols in a Brazilian agro-industrial area: Speciation and impact of biomass burning, Atmos. Res., 271-279, 2016.

Veres, P., Roberts, J. M., Burling, I. R., Warneke, C., de Gouw, J. and Yokelson, R. J.: Measurements of gas-phase inorganic and organic acids from biomass fires by negative-ion proton-transfer chemical-ionization mass spectrometry, J. Geophys Res, 115, D23302, doi:10.1029/2010JD014033, 2010.

Wang, L., Li, X. and Xu, Y.: The Economic Losses Caused By Crop Residues Burnt in Open Field in China, J. Arid Land Resources and Environment, 2, 170-175, 2008a.

Wang, R., Tao, S., Wang, W., Liu, J., Shen, H., Shen, G., Wang, B., Liu, X., Li, W., Huang, Y., Zhang, Y., Lu, Y., Chen, H., Chen, Y., Wang, C., Zhu, D., Wang, X., Li, B., Liu, W., Ma, J. and Prospero, A.: Black carbon emissions in China from 1949 to 2050, Environ. Sci. Technol., 14, 7595-7603, 2012.

Wang, S. and Zhang, C.: Spatial and temporal distribution of air pollutant emissions from open burning

of crop residues in China, Sciencepaper Online, 5:329-333, 2008b.(*in chinese*)
Wang, S., Zhao, M., Xing, J., Wu, Y., Zhou, Y., Lei, Y., He, K., Fu, L. and Hao, J.: Quantifying the air pollutants emission reduction during the 2008 Olympic Games in Beijing, Environ. Sci. Technol., 7, 2490-2496, 2010.
Wang, W., Jariyasopit, N., Schrlau, J., Jia, Y., Tao, S., Yu, T., Dashwood, R. H., Zhang, W., Wang, X. and Simonich, S.: Concentration and photochemistry of PAHs, NPAHs, and OPAHs and toxicity of $PM_{2.5}$ during the Beijing Olympic Games, Environ. Sci. Technol., 16, 6887-6895, 2011.
Wei, B. and Yang, L.: A review of heavy metal contaminations in urban soils, urban road dusts and agricultural soils from China, Microchem J., 2, 99-107, 2010.
Wei, W., Jitao, Y., Qingling, Z. and Bailiang, Z.: Current Situation and Developing Direction of Straw Utilization Technology in China, China Resources Comprehensive Utilization, 11, 2004.
WHO, Life Database in 2000, World Health Organization, 2000.
Wilson, J. M., Baeza-Romero, M. T., Jones, J. M., Pourkashanian, M., Williams, A., Lea-Langton, A. R., Ross, A. B. and Bartle, K.: Soot Formation from the Combustion of Biomass Pyrolysis Products and a Hydrocarbon Fuel, n-Decane: An Aerosol Time Of Flight Mass Spectrometer (ATOFMS) Study, Energ Fuel, 3, 1668-1678, 2013.
Wong, C., Vichit-Vadakan, N., Kan, H., Qian, Z. and Teams, T. P. P.: Public Health and Air Pollution in Asia (PAPA): A Multicity Study of Short-Term Effects of Air Pollution on Mortality, Environ. Health Persp., 9, 1195-1202, 2008.
Wu, C., Liu, L. J. S., Cullen, A., Westberg, H. and Williamson, J., Spatial-temporal and cancer risk assessment of selected hazardous air pollutants in Seattle, Environ Int., 1, 11-17, 2011.
Wu, C., Wu, S., Wu, Y., Cullen, A. C., Larson, T. V., Williamson, J. and Liu, L. J. S.: Cancer risk assessment of selected hazardous air pollutants in Seattle, Environ Int., 3, 516-522, 2009.
Xu, S., Liu, W. and Tao, S.: Emission of Polycyclic Aromatic Hydrocarbons in China, Environ Sci. Technol., 3, 702-708, 2006.
Yang, C., Peng, X., Huang, W., Chen, R., Xu, Z., Chen, B. and Kan, H. . A time-stratified case-crossover study of fine particulate matter air pollution and mortality in Guangzhou, China, Int Arch. Occ. Env. Hea., 5, 579-585, 2012.
Yang, M., Howell, S. G., Zhuang, J. and Huebert, B. J.: Attribution of aerosol light absorption to black carbon, brown carbon, and dust in China-interpretations of atmospheric measurements during EAST-AIRE, Atmos. Chem. Phys., 6, 2035-2050, doi:10.5194/acp-9-2035-2009, 2009.
Yang, Y., Liu, X., Qu, Y., Wang, J., An, J., Zhang, Y. and Zhang, F.: Formation mechanism of continuous extreme haze episodes in the megacity Beijing, China, in January 2013, Atmos. Res., 192-203, 2015.
Yokelson, R. J., Karl, T., Artaxo, P. and Blake, D. R.: The Tropical Forest and Fire Emissions Experiment: overview and airborne fire emission factor measurements, Atmos. Chem. Phys., 7, 5175-5196, doi:10.5194/acp-7-5175-2007, 2007.
Yunker, M. B., Macdonald, R. W., Vingarzan, R., Mitchell, R. H., Goyette, D. and Sylvestre, S.: PAHs in the Fraser River basin: a critical appraisal of PAH ratios as indicators of PAH source and composition, Org Geochem, 4, 489-515, 2002.
Zhang, H., Hu, D., Chen, J., Ye, X., Wang, S. X., Hao, J. M., Wang, L., Zhang, R. and An, Z.: Particle Size Distribution and Polycyclic Aromatic Hydrocarbons Emissions from Agricultural Crop Residue Burning, Environ. Sci. Technol., 13, 5477-5482, 2011.
Zhang, H., Wang, S., Hao, J., Wan, L., Jiang, J., Zhang, M., Mestl, H. E., Mestl, H., Alnes, L., Aunan, K.

and Mellouki, A.: Chemical and size characterization of particles emitted from the burning of coal and wood in rural households in Guizhou, China, Atmos. Environ., 94-99, 2012.

Zhang, H., Ye, X., Cheng, T., Chen, J., Yang, X., Wang, L. and Zhang, R.: A laboratory study of agricultural crop residue combustion in China: Emission factors and emission inventory, Atmos. Environ., 36, 8432-8441, 2008a.

Zhang, R., Khalizov, A. F., Pagels, J., Zhang, D., Xue, H. and McMurry, P. H.: Variability in morphology, hygroscopicity, and optical properties of soot aerosols during atmospheric processing, Proc Natl Acad Sci USA, 30, 10291-10296, 2008b.

Zhang, R., Suh, I., Zhao, J., Zhang, D., Fortner, E. C., Tie, X., Molina, L. T. and Molina, M. J.: Atmospheric new particle formation enhanced by organic acids, Science, 5676, 1487-1490, 2004.

Zhao, B., Wang, P., Ma, J. Z., Zhu, S., Pozzer, A. and Li, W.: A high-resolution emission inventory of primary pollutants for the Huabei region, China, Atmos. Chem. Phys., 1, 481-501, 2012.

Zhao, Y., Nielsen, C. P., Lei, Y., McElroy, M. B. and Hao, J.: Quantifying the Uncertainties of a Bottom-Up Emission Inventory of Anthropogenic Atmospheric Pollutants in China, Atmos. Chem. Phys., 11, 2295-2308, 2011.

Zheng, J., Ma, Y., Chen, M., Zhang, Q., Wang, L., Khalizov, A. F., Yao, L., Wang, Z., Wang, X. and Chen, L.: Measurement of atmospheric amines and ammonia using the high resolution time-of-flight chemical ionization mass spectrometry, 249-259, 2015.

Table and figure captions

Table 1. Emission factors of particulate chemical species in smoke $PM_{2.5}$ from agricultural residue burning (mean value ± standard deviation).

Table 2. Emission factors of particulate chemical species in smoke $PM_{1.0}$ from agricultural residue burning (mean value ± standard deviation).

Table 3. Comparison of emission factors with literature (specific chemical materials in form of $PM_{2.5}$)

Table 4. Summary of field burning rates and economic data in China

Table 5. National agricultural field burning emissions of BAU, EM, and NDRC scenarios in China, 2012.

Table 6. Uncertainties for national smoke aerosol emissions in 2012**.**

Table 7. Estimated number of cases (95% CI) attributable to agricultural fire smoke $PM_{2.5}$ exposure in China, 2012

Table 8. Health-related economic loss (95% CI) from agricultural fire smoke $PM_{2.5}$ exposure in China, 2012

Figure 1. Schematic methodology for developing emission estimations

Figure 2. Chemical profiles of smoke $PM_{2.5}$ and $PM_{1.0}$ from 5 types agricultural residue burnings. OM (organic matter = 1.3×OC). OWSI, other water soluble ions including F^-, NO_2^-, Na^+, Ca^{2+}, Mg^{2+}.

Figure 3. a) Emission factors of 16 USEPA priority PAHs in smoke $PM_{2.5}$ and $PM_{1.0}$; b) expulsion-accumulation of PAHs in OC-EC of smoke $PM_{2.5}$ and $PM_{1.0}$

Figure 4. Transmission electron microscope (TEM) images and EDX analysis of fresh agricultural residue burning particles. (a)-(c) Crystal and amorphous KCl particles internally mixed with sulfate, nitrate, and carbonaceous materials. (d)-(f) Heavy metal-bearing fractal-like fly ash particles. (e)-(g) Chain-like soot particles and tar ball.

Figure 5. Annual agricultural residue production of five major crops and allocated into two harvest (summer and autumn harvest) based on agricultural yield in China, 2012.

Figure 6. Statistical analysis of field burning rates from BAU, EM, and NDRC versions

Figure 7. Spatial and temporal distribution of smoke $PM_{2.5}$ emissions and flux concentrations from agricultural field burning over China, 2012

Figure 8. Nationwide $PM_{2.5}$ emissions and flux concentrations based on different burning versions. The inset pie-graphs are chemical compositions of integrated $PM_{2.5}$

1609 from five major agricultural residue burning.

1610

1611 **Table 1.** Emission factors of particulate chemical species in smoke $PM_{2.5}$ from
1612 agricultural residue burning (mean value ± standard deviation).

Chemical Species (g kg^{-1})	wheat straw	corn straw	rice straw	cotton residue	soybean residue
$PM_{2.5}$	5.803 ± 0.363	5.988 ± 0.723	14.732 ± 2.417	15.162 ± 2.053	3.249 ± 0.350
OC	2.813 ± 0.147	2.393 ± 0.351	6.882 ± 0.689	7.415 ± 0.547	1.539 ± 0.253
EC	0.676 ± 0.027	0.778 ± 0.152	2.182 ± 0.278	1.192 ± 0.171	0.614 ± 0.190
Inorganic ions (g kg^{-1})	**1.273 ± 0.072**	**1.810 ± 0.030**	**3.086 ± 0.266**	**3.810 ± 0.246**	**0.523 ± 0.149**
SO_4^{2-}	0.084 ± 0.028	0.217 ± 0.041	0.409 ± 0.127	0.701 ± 0.081	0.073 ± 0.014
Cl^-	0.576 ± 0.038	0.709 ± 0.034	1.158 ± 0.232	1.351 ± 0.114	0.178 ± 0.030
F^-	0.023 ± 0.061	0.061 ± 0.005	0.073 ± 0.024	0.265 ± 0.012	0.009 ± 0.004
NO_3^-	0.023 ± 0.000	0.032 ± 0.002	0.051 ± 0.025	0.072 ± 0.004	0.009 ± 0.004
NO_2^-	0.006 ± 0.001	0.016 ± 0.002	0.018 ± 0.002	0.036 ± 0.001	0.004 ± 0.003
Ca^{2+}	0.030 ± 0.011	0.036 ± 0.003	0.046 ± 0.007	0.060 ± 0.003	0.010 ± 0.002
Na^+	0.005 ± 0.001	0.012 ± 0.001	0.028 ± 0.004	0.050 ± 0.004	0.005 ± 0.001
NH_4^+	0.152 ± 0.005	0.197 ± 0.010	0.542 ± 0.107	0.347 ± 0.008	0.029 ± 0.004
Mg^{2+}	0.005 ± 0.000	0.017 ± 0.002	0.023 ± 0.004	0.032 ± 0.002	0.005 ± 0.001
K^+	0.368 ± 0.041	0.514 ± 0.009	0.739 ± 0.049	0.947 ± 0.070	0.200 ± 0.023
Organic Acids (mg kg^{-1})	**156.680 ± 81.830**	**46.670 ± 9.000**	**557.130 ± 269.380**	**769.990 ± 317.550**	**143.310 ± 39.770**
CH_3COOH	148.900 ± 79.290	36.640 ± 8.210	417.930 ± 186.140	743.320 ± 159.600	135.500 ± 62.320
MSA	7.170 ± 2.110	10.030 ± 30.000	136.990 ± 81.700	12.980 ± 1.530	3.200 ± 1.530
$H_2C_2O_4$	2.610 ± 0.430	ND	2.210 ± 1.560	4.760 ± 2.640	2.170 ± 2.380
HCOOH	ND	ND	ND	8.930 ± 2.630	2.440 ± 1.450
Amine salts (mg kg^{-1})	**19.246 ± 9.368**	**32.877 ± 19.141**	**104.787 ± 15.635**	**102.409 ± 13.379**	**4.514 ± 1.776**
$MeOH^+$ + $MMAH^+$	1.322 ± 0.086	5.735 ± 0.102	17.226 ± 1.454	19.888 ± 0.351	0.456 ± 0.196
$MEAH^+$	0.201 ± 0.055	0.675 ± 0.135	4.175 ± 0.920	3.690 ± 1.959	ND
$TEOH^+$	2.562 ± 0.962	4.118 ± 0.741	25.129 ± 0.343	14.376 ± 8.688	0.672 ± 0.558
$DEAH^+$ + $TMAH^+$	13.728 ± 7.512	18.973 ± 0.466	46.148 ± 12.185	28.568 ± 5.321	2.012 ± 0.878
$DMAH^+$	1.434 ± 0.925	3.376 ± 0.674	12.110 ± 6.166	35.887 ± 2.940	1.374 ± 0.144
Elemental Species (mg kg^{-1})	**53.813 ± 18.860**	**53.546 ± 9.070**	**131.612 ± 5.920**	**27.577 ± 3.700**	**14.003 ± 8.710**
Phenols (mg kg^{-1})	**26.785 ± 8.582**	**16.390 ± 2.652**	**27.238 ± 4.861**	**41.481 ± 5.517**	**9.673 ± 2.272**
PAHs (mg kg^{-1})	**1.814 ± 0.348**	**2.706 ± 0.798**	**7.267 ± 1.722**	**8.302 ± 2.856**	**1.832 ± 0.353**

1613 *ND means not detected*

Table 2. Emission factors of particulate chemical species in smoke $PM_{1.0}$ from agricultural residue burning (mean value ± standard deviation).

Chemical Species (g kg^{-1})	wheat straw	corn straw	rice straw	cotton residue	soybean residue
$PM_{1.0}$	5.298 ± 0.295	5.360 ± 0.551	13.200 ± 1.440	12.635 ± 1.243	3.036 ± 0.257
OC	2.419 ± 0.126	2.063 ± 0.340	6.024 ± 0.602	6.036 ± 0.360	1.338 ± 0.128
EC	0.650 ± 0.037	0.728 ± 0.122	2.083 ± 0.413	1.023 ± 0.205	0.575 ± 0.260
Inorganic ions (g kg^{-1})	**1.215 ± 0.040**	**1.768 ± 0.010**	**2.940 ± 0.249**	**3.516 ± 0.145**	**0.510 ± 0.156**
SO_4^{2-}	0.078 ± 0.011	0.199 ± 0.032	0.333 ± 0.107	0.581 ± 0.054	0.073 ± 0.056
Cl^-	0.544 ± 0.033	0.712 ± 0.027	1.145 ± 0.118	1.243 ± 0.067	0.175 ± 0.031
F^-	0.022 ± 0.007	0.041 ± 0.004	0.078 ± 0.030	0.151 ± 0.011	0.001 ± 0.001
NO_3^-	0.021 ± 0.005	0.027 ± 0.002	0.043 ± 0.016	0.061 ± 0.003	0.009 ± 0.002
NO_2^-	0.006 ± 0.001	0.010 ± 0.003	0.013 ± 0.004	0.019 ± 0.002	0.004 ± 0.003
Ca^{2+}	0.027 ± 0.013	0.028 ± 0.002	0.045 ± 0.008	0.067 ± 0.005	0.010 ± 0.002
Na^+	0.004 ± 0.000	0.012 ± 0.000	0.027 ± 0.003	0.056 ± 0.006	0.005 ± 0.002
NH_4^+	0.147 ± 0.005	0.191 ± 0.009	0.511 ± 0.067	0.401 ± 0.004	0.031 ± 0.005
Mg^{2+}	0.005 ± 0.001	0.035 ± 0.001	0.024 ± 0.006	0.033 ± 0.002	0.005 ± 0.001
K^+	0.359 ± 0.040	0.513 ± 0.015	0.721 ± 0.073	0.994 ± 0.067	0.197 ± 0.035
Organic Acids (mg kg^{-1})	**124.310 ± 25.170**	**47.830 ± 10.610**	**427.400 ± 221.270**	**639.820 ± 244.960**	**130.760 ± 59.310**
CH_3COOH	115.790 ± 21.940	38.960 ± 9.610	383.360 ± 179.050	615.790 ± 232.860	124.310 ± 69.000
MSA	6.830 ± 2.030	8.870 ± 2.730	41.380 ± 38.480	11.380 ± 2.360	3.200 ± 1.730
$H_2C_2O_4$	1.690 ± 1.200	ND	2.660 ± 1.760	3.620 ± 1.250	1.560 ± 1.670
HCOOH	ND	ND	ND	9.030 ± 7.710	1.690 ± 1.390
Amine salts (mg kg^{-1})	**18.191 ± 5.351**	**29.891 ± 13.480**	**81.726 ± 11.455**	**85.720 ± 21.337**	**4.385 ± 1.445**
$MeOH^+$ + $MMAH^+$	1.300 ± 0.282	5.647 ± 0.342	16.627 ± 0.104	18.834 ± 1.991	0.464 ± 0.265
$MEAH^+$	0.157 ± 0.037	0.787 ± 0.211	3.581 ± 0.602	2.771 ± 1.304	ND
$TEOH^+$	1.719 ± 0.283	5.115 ± 0.732	17.575 ± 0.844	11.441 ± 3.229	0.529 ± 0.304
$DEAH^+$ + $TMAH^+$	13.716 ± 9.047	15.921 ± 1.620	33.565 ± 6.795	29.057 ± 3.793	2.278 ± 0.533
$DMAH^+$	1.300 ± 0.702	2.420 ± 0.575	10.377 ± 4.521	23.617 ± 20.086	1.115 ± 0.343
Elemental Species (mg kg^{-1})	**31.586 ± 10.630**	**29.265 ± 4.240**	**51.062 ± 5.920**	**16.738 ± 3.480**	**11.817 ± 6.650**
Phenols (mg kg^{-1})	**20.774 ± 4.972**	**13.193 ± 2.181**	**20.480 ± 1.403**	**23.521 ± 8.521**	**7.689 ± 1.356**
PAHs (mg kg^{-1})	**1.257 ± 0.398**	**1.420 ± 0.232**	**3.967 ± 0.970**	**4.359 ± 1.373**	**1.123 ± 0.205**

ND means not detected

Table 3. Comparison of emission factors with literature (specific chemical materials in form of $PM_{2.5}$).

Species	Emission factors (g kg^{-1})		Reference
	This work	Reference value	
$PM_{2.5}$	8.99 ± 5.55	7.6~11.7(AR), 6.26~15.3 (TL), ~3.0 (AR), 2.2~15.0 (AR)	Li et al., 2007; Akagi et al., 2011; Dhammapala et al., 2007; Hayashi et al., 2014
$PM_{1.0}$	7.91 ± 4.67	4.4.3~12.1 (TL)	May et al., 2014
OC	4.21 ± 2.73	2.7~3.9 (AR), 2.3~9.7(TL), ~1.9(AR) , 1.0~9.3 (AR), 0.8~5.9 (TL)	Li et al., 2007; Akagi et al., 2011; Dhammapala et al., 2007; Hayashi et al., 2014; May et al., 2014
EC	1.09 ± 0.65	0.35~0.49 (AR), 0.37~0.91(TL), ~0.4(AR), 0.21~0.81(AR), 1.13~1.73 (TL)	Li et al., 2007; Akagi et al., 2011; Dhammapala et al., 2007; Hayashi et al., 2014; May et al., 2014
WSOA	0.33 ± 0.31	0.039~0.109 (TL)	Akagi et al., 2011
WSA	0.05 ± 0.05	0.08~0.13 (TL), ~0.55 (TL)	Akagi et al., 2011; Andreae et al., 2001
WSI	2.10 ± 1.34	1.84~4.9 (AR),0.8~1.31(TL), 0.43~1.63 (AR)	Li et al., 2007; Akagi et al., 2011; Hayashi et al., 2014
THM	0.06 ± 0.05	0.06~0.09 (AR)	Li et al., 2007
PAHs ($\times 10^3$)	4.38 ± 3.15	~17(AR), 0.72~1.64(AR), ~9.0 (W)	Dhammapala et al., 2007; Zhang et al., 2011; Lee et al.2005
Phenols ($\times 10^3$)	24.31 ± 12.11	~35(AR), ~5 (AR), ~13 (TL)	Dhammapala et al., 2007; Hays et al., 2005; Andreae et al., 2001

AR: agricultural residue; TL: total, including forest fires and straw burning; W: wood

Table 4. Summary of field burning rates and economic data in China.

Province	Burning rate from literature		Agricultural income ratio [c]			Estimated burning rate		NDRC report [d]	Average rate
	BAU-I [a]	BAU-II [b]	2000	2006	2012	EM-I	EM-II	NDRC	
Beijing	0.00	0.17	0.08	0.06	0.06	0.00	0.19	0.13	0.10 ± 0.08
Tianjin	0.00	0.17	0.10	0.14	0.12	0.00	0.20	0.30	0.13 ± 0.12
Hebei	0.20	0.17	0.27	0.22	0.24	0.22	0.16	0.19	0.19 ± 0.02
Shanxi	0.20	0.17	0.20	0.21	0.25	0.16	0.14	0.22	0.18 ± 0.03
Inner Mongolia	0.00	0.12	0.44	0.49	0.66	0.00	0.09	0.27	0.10 ± 0.10
Liaoning	0.20	0.12	0.30	0.29	0.39	0.16	0.09	0.34	0.18 ± 0.09
Jilin	0.30	0.12	0.73	0.73	0.77	0.28	0.11	0.25	0.21 ± 0.08
Heilongjiang	0.30	0.12	0.99	0.83	0.59	0.50	0.17	0.25	0.27 ± 0.13
Shanghai	0.00	0.32	0.10	0.08	0.09	0.00	0.29	0.12	0.15 ± 0.14
Jiangsu	0.30	0.32	0.32	0.22	0.30	0.32	0.23	0.19	0.27 ± 0.05
Zhejiang	0.30	0.32	0.19	0.08	0.09	0.64	0.28	0.22	0.35 ± 0.15
Anhui	0.20	0.32	0.44	0.39	0.43	0.21	0.29	0.43	0.29 ± 0.08
Fujian	0.30	0.32	0.18	0.10	0.14	0.39	0.22	0.17	0.28 ± 0.08
Jiangxi	0.20	0.11	0.45	0.31	0.44	0.20	0.08	0.25	0.17 ± 0.06
Shandong	0.30	0.17	0.33	0.25	0.24	0.40	0.17	0.21	0.25 ± 0.09
Henan	0.20	0.17	0.39	0.35	0.33	0.23	0.18	0.22	0.20 ± 0.02
Hubei	0.20	0.11	0.42	0.30	0.41	0.21	0.08	0.30	0.18 ± 0.08
Hunan	0.20	0.33	0.47	0.31	0.43	0.22	0.24	0.35	0.27 ± 0.06
Guangdong	0.30	0.33	0.19	0.10	0.13	0.44	0.25	0.18	0.30 ± 0.09
Guangxi	0.20	0.33	0.40	0.25	0.33	0.25	0.25	0.35	0.28 ± 0.06
Hainan	0.30	0.33	0.35	0.16	0.21	0.51	0.25	0.56	0.39 ± 0.12
Chongqing	0.20	0.11	0.35	0.23	0.30	0.24	0.08	0.45	0.22 ± 0.13
Sichuan	0.20	0.11	0.37	0.22	0.28	0.26	0.09	0.30	0.19 ± 0.08
Guizhou	0.20	0.11	0.38	0.23	0.25	0.31	0.10	0.43	0.23 ± 0.13
Yunnan	0.20	0.11	0.36	0.26	0.31	0.24	0.09	0.28	0.18 ± 0.07
Tibet	0.00	0.16	0.15	0.09	0.05	0.00	0.30	0.16	0.12 ± 0.11
Shannxi	0.20	0.17	0.33	0.27	0.26	0.25	0.18	0.28	0.22 ± 0.04
Gansu	0.10	0.16	0.25	0.20	0.28	0.09	0.11	0.33	0.16 ± 0.09
Qinghai	0.00	0.16	0.23	0.10	0.08	0.00	0.20	0.28	0.13 ± 0.11
Ningxia	0.10	0.16	0.42	0.38	0.45	0.09	0.13	0.16	0.13 ± 0.03
Xinjiang	0.10	0.16	0.43	0.61	0.73	0.06	0.13	0.30	0.15 ± 0.08
Nationwide	**0.21**	**0.16**	**0.34**	**0.27**	**0.31**	**0.26**	**0.15**	**0.27**	**0.21 ± 0.05**

a. Zhao et al., 2012; Cao et al., 2006; Cao et al., 2011

b. Wang and Zhang., 2008

c. Calculated based on data from China Yearbook 2001~2013 (NBSC, 2001-2013), China Rural Statistic Yearbook 2001~2013, data available at http://www.grain.gov.cn/Grain/

d. *Data from the National Development and Reform Commission report ([2014]No.516) : http://www.sdpc.gov.cn/*

Table 5. National agricultural field burning emissions of BAU, EM, and NDRC scenarios in China in 2012.

Unit: Gg	BAU-I			BAU-II			EM-1			EM-2			NDRC			Average		
	Total	Summer	Autumn	Total	Summer	Autumn	Total	Summer	Autumn	Total	Summer	Autumn	Total	Summer	Autumn	Total	Summer	Autumn
$PM_{2.5}$	1001.05	218.99	782.06	835.42	209.29	626.13	1211.92	258.58	953.34	738.36	182.34	556.02	1241.69	258.24	983.46	1007.650	226.007	781.646
$PM_{1.0}$	897.52	198.93	698.59	748.57	189.92	558.65	1087.05	234.85	852.20	661.81	165.61	496.20	1111.90	234.44	877.46	903.125	205.217	697.911
OC	429.51	102.87	326.64	360.99	97.67	263.32	519.26	121.33	397.94	318.84	85.55	233.29	533.19	120.86	412.33	433.184	105.885	327.300
EC	133.61	27.37	106.24	111.40	26.52	84.88	162.71	32.39	130.32	98.06	22.85	75.21	164.97	32.53	132.45	134.414	28.404	106.010
SO_4^{2-}	30.22	3.96	26.26	24.97	3.94	21.04	36.39	4.71	31.68	22.09	3.32	18.76	38.21	4.78	33.44	30.440	4.155	26.285
NO_3^-	4.35	0.84	3.51	3.55	0.80	2.75	5.24	0.99	4.25	3.17	0.70	2.47	5.40	0.99	4.41	4.350	0.864	3.486
NH_4^+	32.08	6.37	25.71	26.65	6.21	20.44	39.09	7.54	31.55	23.43	5.32	18.11	39.46	7.59	31.87	32.202	6.623	25.580
K^+	67.49	13.12	54.38	54.75	12.38	42.37	81.40	15.45	65.95	49.10	10.90	38.20	83.62	15.36	68.26	67.412	13.469	53.943
WSOA	24.44	6.55	17.89	21.94	6.39	15.55	29.69	7.76	21.93	18.77	5.48	13.30	30.82	7.81	23.01	25.174	6.815	18.360
WSA	5.75	0.95	4.80	4.85	0.95	3.90	6.99	1.13	5.86	4.23	0.80	3.43	7.19	1.15	6.04	5.815	1.000	4.815
PAHs	0.48	0.11	0.37	0.40	0.10	0.30	0.58	0.12	0.45	0.35	0.09	0.26	0.59	0.13	0.47	0.480	0.109	0.371
Phenols	2.71	0.85	1.87	2.25	0.78	1.47	3.25	0.99	2.26	2.02	0.70	1.323	3.40	0.98	2.36	2.721	0.861	1.861
THM	8.68	2.01	6.67	7.19	1.92	5.27	10.56	2.37	8.19	6.36	1.67	4.69	10.64	2.37	8.27	8.702	2.073	6.628
WSI	249.96	47.46	202.50	204.46	45.24	159.22	301.75	56.01	245.74	182.31	39.50	142.82	310.31	55.88	254.43	250.269	48.927	201.342

Table 6. Uncertainties for the national smoke aerosol emissions in 2012 (pollutant emission in unit of Gg/yr, 95% CI in percentage)

Species	BAU-I		BAU-II		EM-I		EM-II		NDRC		Average	
$PM_{2.5}$	1001.1	(-52.3% , 73.5%)	835.4	(-48.7% , 68.8%)	1211.9	(-63.6% , 84.3%)	738.4	(-55.9% , 74.3%)	1241.7	(-46.2% , 65.1%)	1005.7	(-24.6% , 33.7%)
$PM_{1.0}$	897.5	(-51.6% , 73.0%)	748.6	(-48.4% , 68.6%)	1087.1	(-62.9% , 83.8%)	661.8	(-55.5% , 74.1%)	1111.9	(-45.7% , 64.7%)	901.4	(-24.4% , 33.5%)
OC	429.5	(-50.5% , 71.5%)	361.0	(-48.9% , 69.2%)	519.3	(-61.4% , 81.8%)	318.8	(-55.6% , 74.1%)	533.2	(-47.1% , 66.7%)	432.4	(-24.2% , 33.3%)
EC	133.6	(-52.1% , 73.6%)	111.4	(-50.1% , 71.0%)	162.7	(-63.3% , 84.3%)	98.1	(-56.8% , 75.7%)	165.0	(-46.7% , 66.0%)	134.2	(-24.8% , 34.0%)
WSOA	24.4	(-68.5% , 86.2%)	21.9	(-75.7% , 95.2%)	29.7	(-78.7% , 96.2%)	18.8	(-77.8% , 95.4%)	30.8	(-67.5% , 85.1%)	25.1	(-33.3% , 41.4%)
WSA	5.8	(-62.8% , 82.1%)	4.9	(-65.9% , 84.1%)	7.0	(-73.9% , 93.2%)	4.2	(-69.3% , 86.3%)	7.2	(-58.7% , 75.9%)	5.8	(-30.1% , 38.5%)
WSI	250.0	(-54.4% , 77.2%)	204.5	(-47.5% , 67.4%)	301.8	(-66.9% , 89.3%)	182.3	(-56.1% , 74.8%)	310.3	(-46.9% , 66.4%)	249.8	(-25.4% , 34.9%)
THM	8.7	(-56.2% , 77.5%)	7.2	(-52.8% , 71.4%)	10.6	(-67.5% , 88.3%)	6.4	(-61.2% , 79.5%)	10.6	(-50.8% , 69.4%)	8.7	(-26.6% , 35.6%)
PAHs	0.5	(-55.2% , 75.7%)	0.4	(-52.4% , 72.2%)	0.6	(-66.5% , 86.8%)	0.4	(-58.8% , 76.9%)	0.6	(-49.3% , 67.8%)	0.5	(-26.0% , 34.9%)
Phenols	2.7	(-56.1% , 77.6%)	2.3	(-51.4% , 70.6%)	3.3	(-67.3% , 88.3%)	2.0	(-59.9% , 78.4%)	3.4	(-48.7% , 67.1%)	2.7	(-26.1% , 35.1%)

Table 7. Estimated number of cases (95% CI) attributable to agricultural fire smoke $PM_{2.5}$ exposure in China, 2012.

Emission version	Mortality	Respiratory hospital admission	Cardiovascular hospital admission	Chronic bronchitis
BAU-I	7864 (3154, 12489)	31123 (21114, 40788)	29454 (12849, 45481)	7577067 (2952006, 11024705)
BAU-II	7187 (3056, 11260)	28711 (19443, 37693)	27156 (11825, 42007)	7132581 (2735111, 10523803)
EM-I	9435 (3817, 14933)	36950 (25151, 48269)	35116 (15373, 54042)	8712880 (3484325, 12430411)
EM-II	6175 (2554, 9751)	25166 (17004, 33112)	23745 (10316, 36816)	6383442 (2407643, 9526727)
NDRC	8523 (3581, 13377)	33957 (23015, 44542)	32131 (14003, 49664)	8332216 (3228351, 12148274)
Average	7836 (3232, 12362)	31181 (21145, 40881)	29520 (12873, 45602)	7267237 (2961487, 1130784)
CRC	538 (227, 850)	2191 (1462, 2920)	2038 (874, 3199)	636650 (214617, 1052153)

Table 8. Health-related economic loss (95% CI) from agricultural fire smoke $PM_{2.5}$ exposure in China, 2012.

Emission version	Economic cost (million US$)				Total cost (million US$)	GDP ratio (‰)
	Mortality	Respiratory hospital admission	Cardiovascular hospital admission	Chronic bronchitis		
BAU-1	1544.5 (730.7, 2430.0)	19.6 (13.3, 25.7)	36.0 (15.7, 55.6)	7187.6 (2800.3, 10458.3)	8787.8 (3560.0, 12969.4)	1.0 (0.4, 1.5)
BAU-2	1453.9 (719, 2252.2)	18.1 (12.2, 23.8)	33.2 (14.4, 51.3)	6766.0 (2594.5, 9982.9)	8271.2 (3340.3, 12310.3)	1.0 (0.4, 1.4)
EM-1	1855.2 (870.3, 2913.7)	23.3 (15.9, 30.5)	42.9 (18.8, 66.1)	8265.0 (3305.2, 11791.5)	10186.5 (4210.2, 14801.8)	1.2 (0.5, 1.7)
EM-2	1228.1 (600.6, 1917.6)	15.9 (10.7, 20.9)	29.0 (12.6, 450)	6055.3 (2283.9, 9037.1)	7328.4 (2907.9, 11020.7)	0.9 (0.3, 1.3)
NDRC	1573.4 (759.3, 2456.2)	21.4 (14.5, 28.1)	39.3 (17.1, 60.7)	7903.9 (3062.4, 11523.9)	9538.2 (3853.4, 14069.0)	1.1 (0.4, 1.6)
Average	1531.0 (736.0, 2393.9)	19.7 (13.3, 25.8)	36.1 (15.7, 55.7)	7235.6 (2809.3, 10558.7)	8822.4 (3574.4, 13034.2)	1.0 (0.4, 1.5)
CRC	100.0 (48.0, 157.1)	1.3 (0.9, 1.8)	2.4 (1.0, 3.9)	603.9 (203.6, 998.1)	707.8 (253.6, 1160.9)	0.1 (0.0, 0.1)

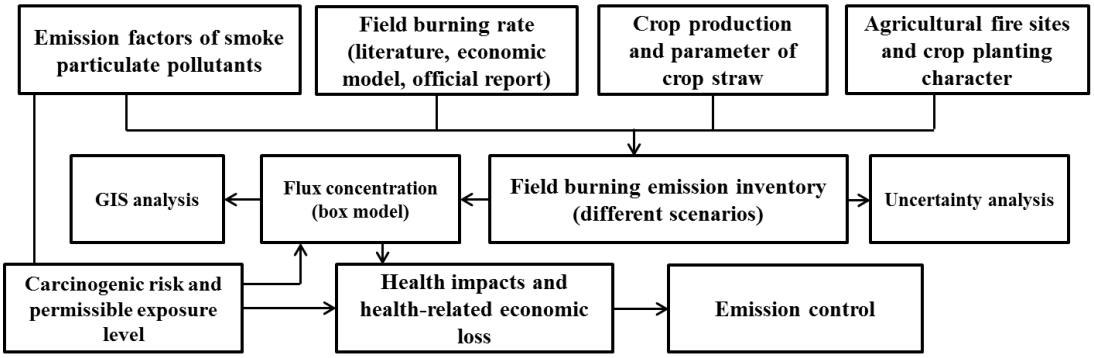

Figure 1. Schematic methodology for developing emission estimations.

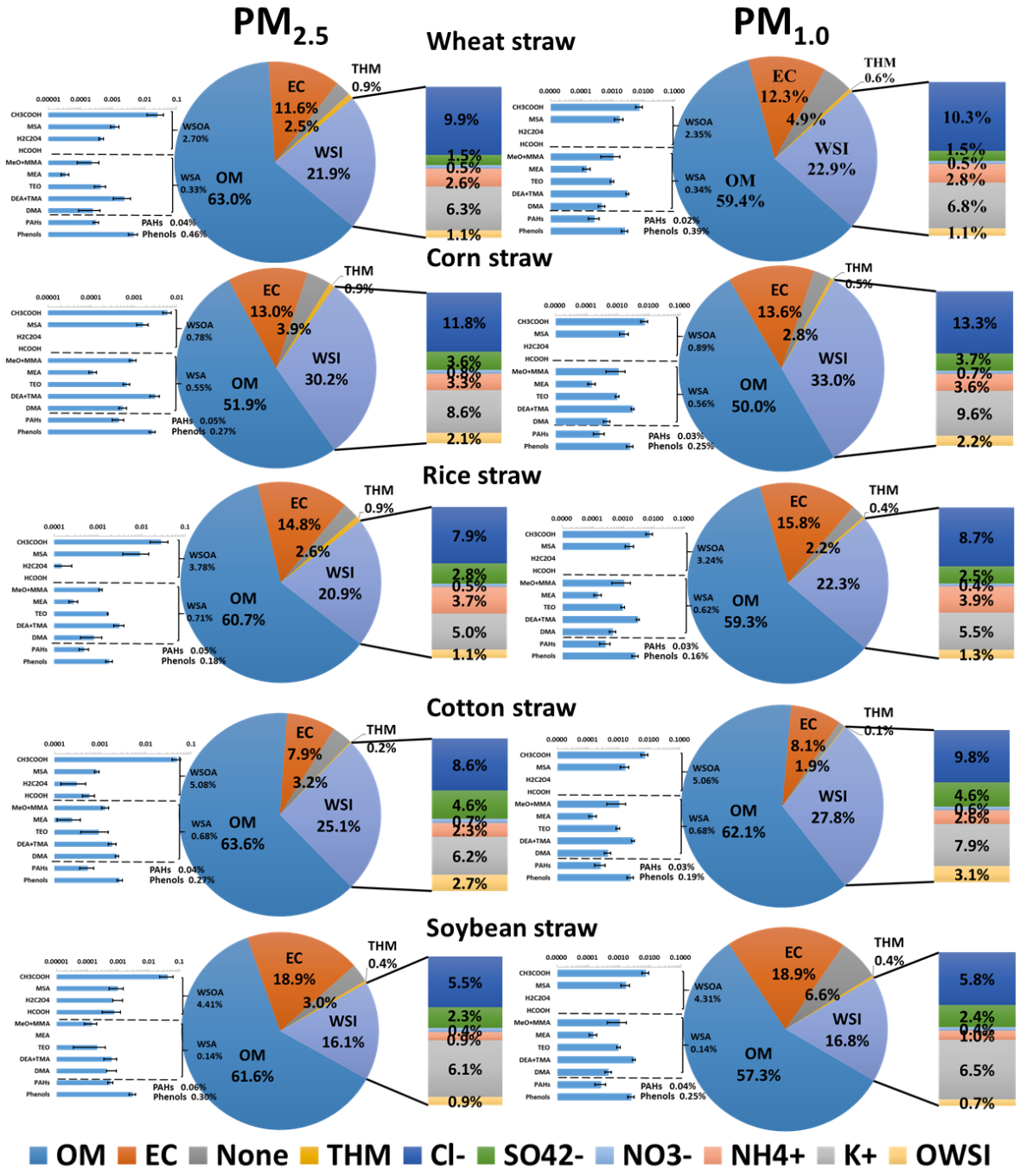

Figure 2. Chemical profiles of smoke $PM_{2.5}$ and $PM_{1.0}$ from 5 types agricultural residue burnings. OM (organic matter = 1.3×OC). OWSI, other water soluble ions including F^-, NO_2^-, Na^+, Ca^{2+}, and Mg^{2+}.

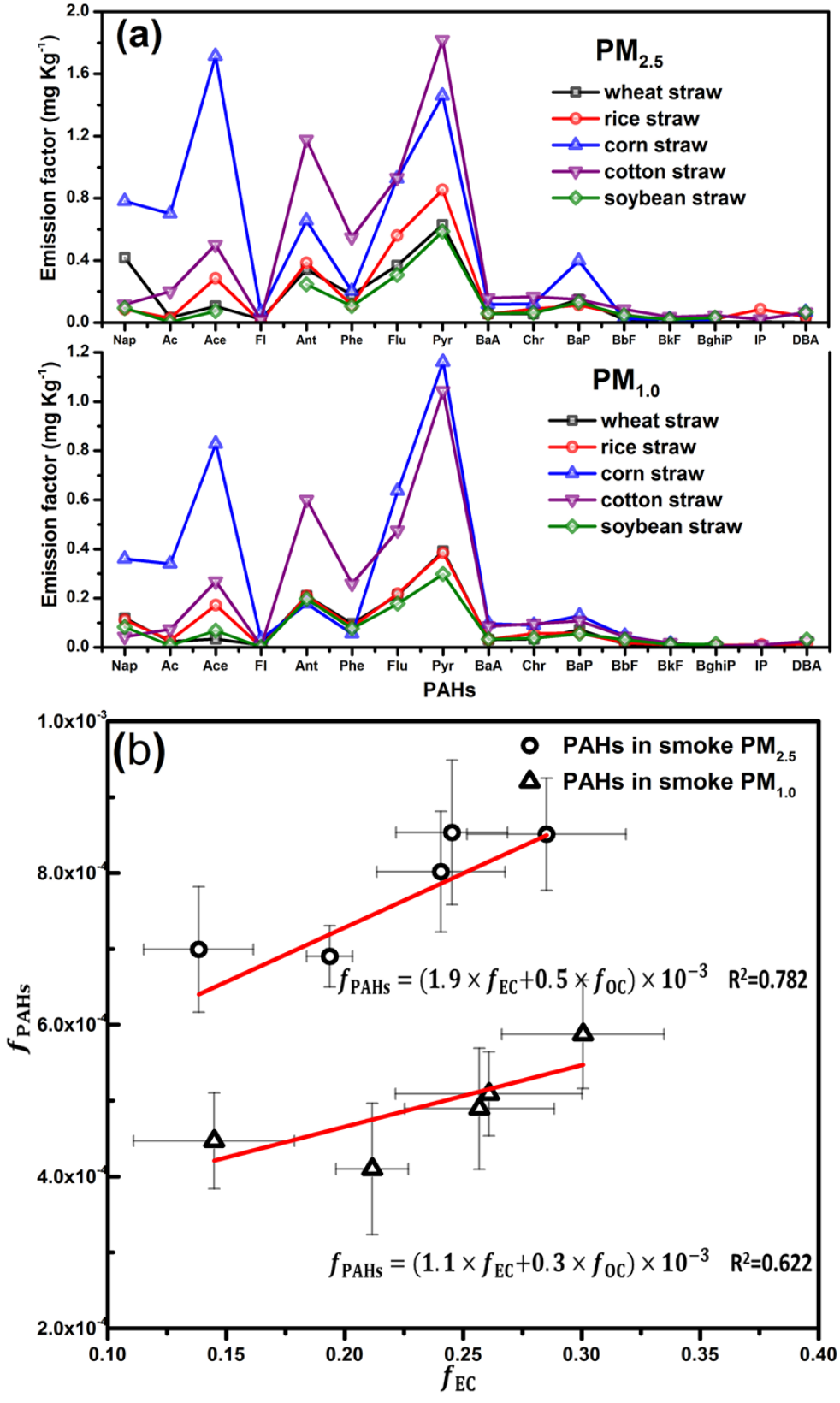

Figure 3. (a) Emission factors of 16 USEPA priority PAHs in smoke $PM_{2.5}$ and $PM_{1.0}$; (b) expulsion-accumulation of PAHs in OC-EC of smoke $PM_{2.5}$ and $PM_{1.0}$.

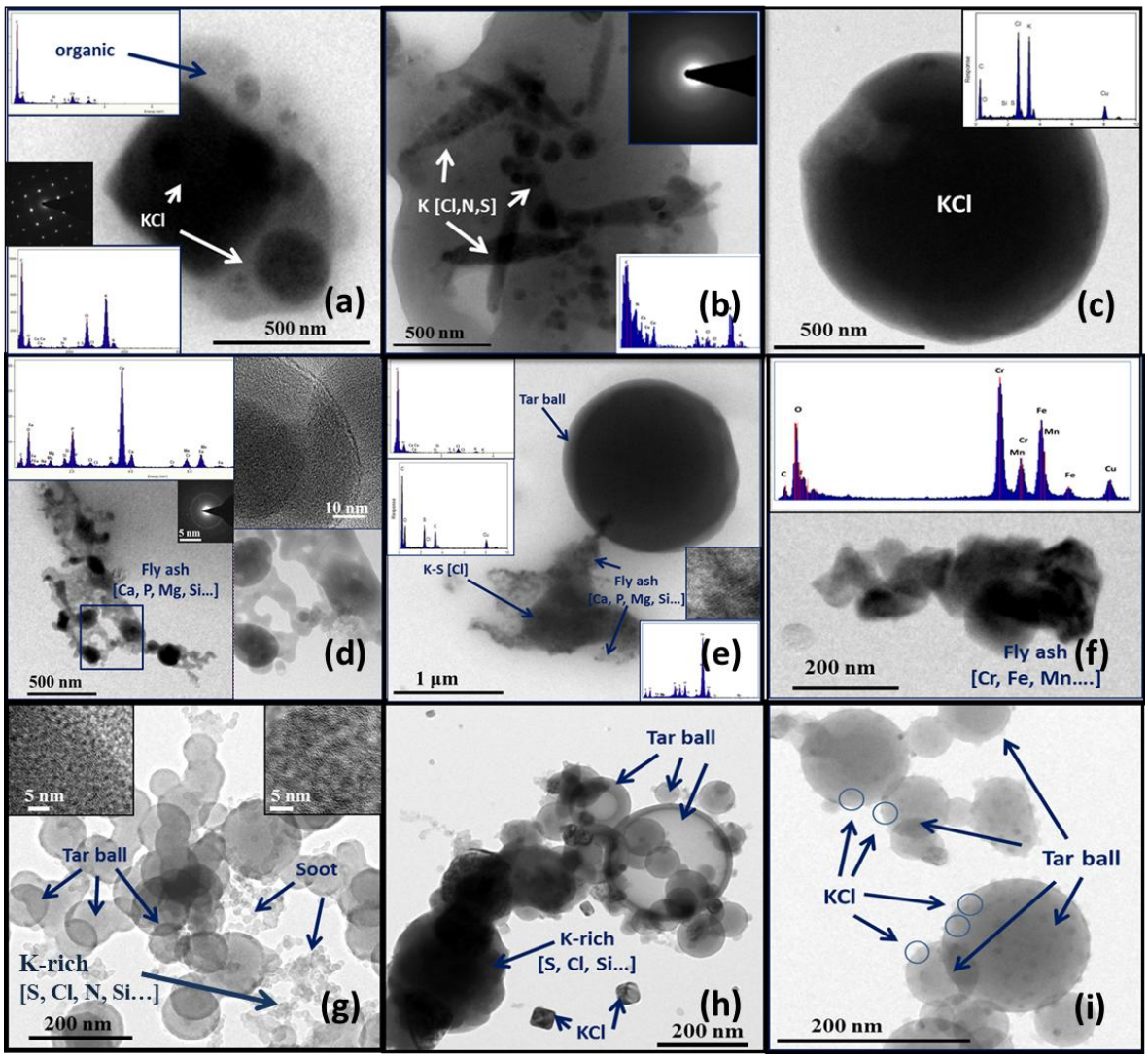

Figure 4. Transmission electron microscope (TEM) images and EDX analysis of fresh agricultural residue burning particles. (a)-(c) Crystal and amorphous KCl particles internally mixed with sulfate, nitrate, and carbonaceous materials. (d)-(f) Heavy metal-bearing fractal-like fly ash particles. (e)-(g) Chain-like soot particles and tar ball.

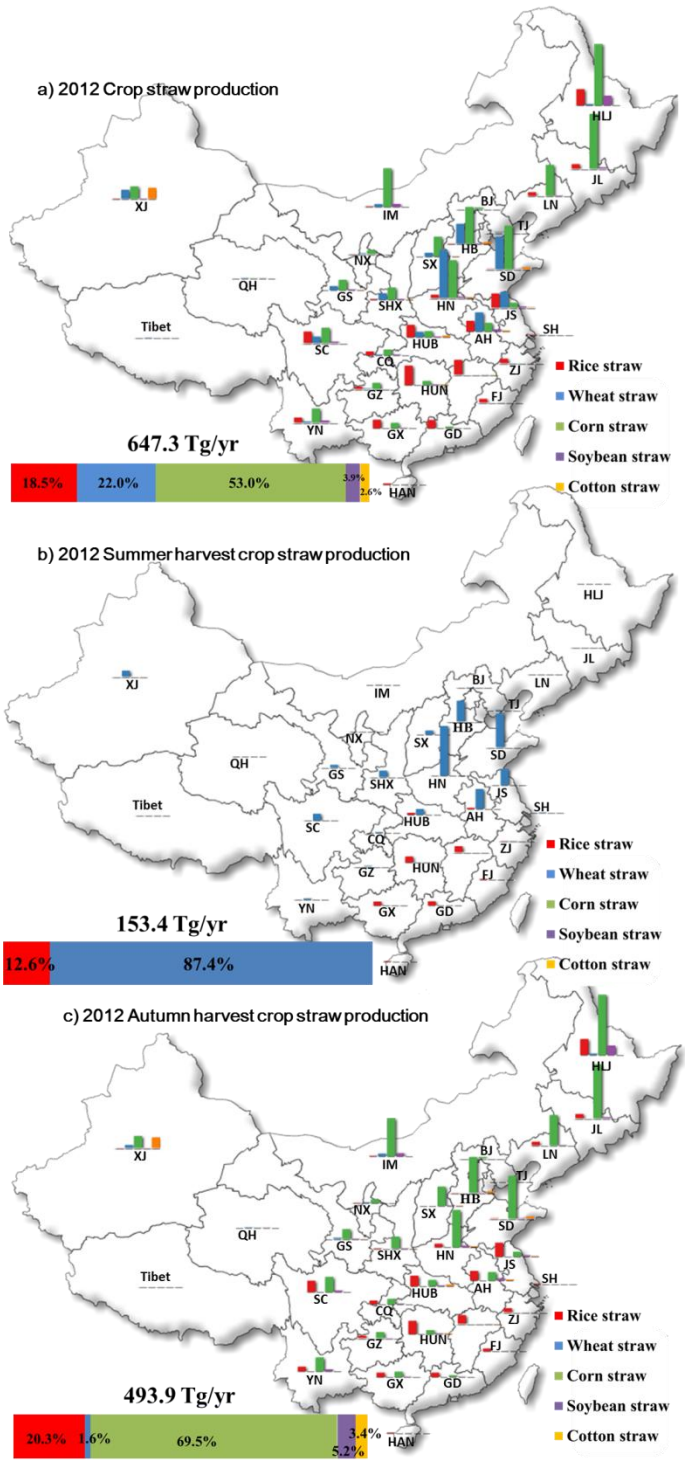

Figure 5. Annual agricultural residue production of five major crops and allocated into two harvest (summer and autumn harvest) based on agricultural yield in China, 2012. (Abbreviation, BJ: Beijing; TJ: Tianjin; HB: Hebei; SX: Shanxi; IM: Inner Mongolia; LN: Liaoning; JL: Jilin; HLJ: Heilongjiang; SH: Shanghai; JS: Jiangsu; ZJ: Zhejiang; AH: Anhui; FJ: Fujian; JX: Jiangxi; SD: Shandong; HN: Henan; HUB: Hubei; HUN: Hunan; GD: Guangdong; GX: Guangxi; HAN: Hainan; CQ: Chongqing; SC: Sichuan; GZ: Guizhou; YN: Yunnan; SHX: Shannxi; GS: Gansu; QH: Qinghai; NX: Ningxia; XJ: Xinjiang)

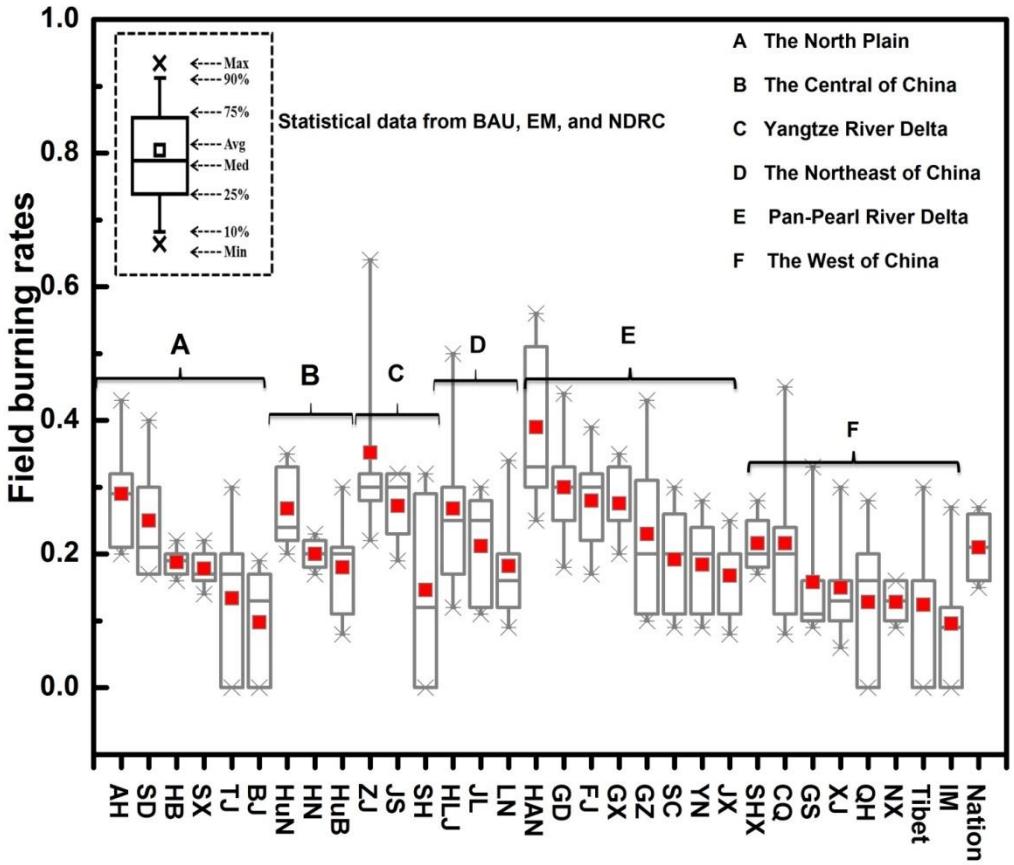

Figure 6. Statistical analysis of field burning rates from BAU, EM, and NDRC versions. The North Plain (Anhui, Shandong, Hebei, Shanxi, Tianjin, Beijing), the Central of China (Hunan, Henan, Hubei), the Yangtze River Delta (Zhejiang, Jiangsu, Shanghai), the Northeast of China (Heilongjiang, Liaoning, Jilin), the Pan-Pearl River Delta (Hainan, Guangdong, Fujian, Guangxi, Guizhou, Sichuan, Yunnan, Jiangxi), the West of China (Shannxi, Chongqing, Xinjiang, Qinghai, Ningxia, Tibet, Inner Mongolia, Gansu)

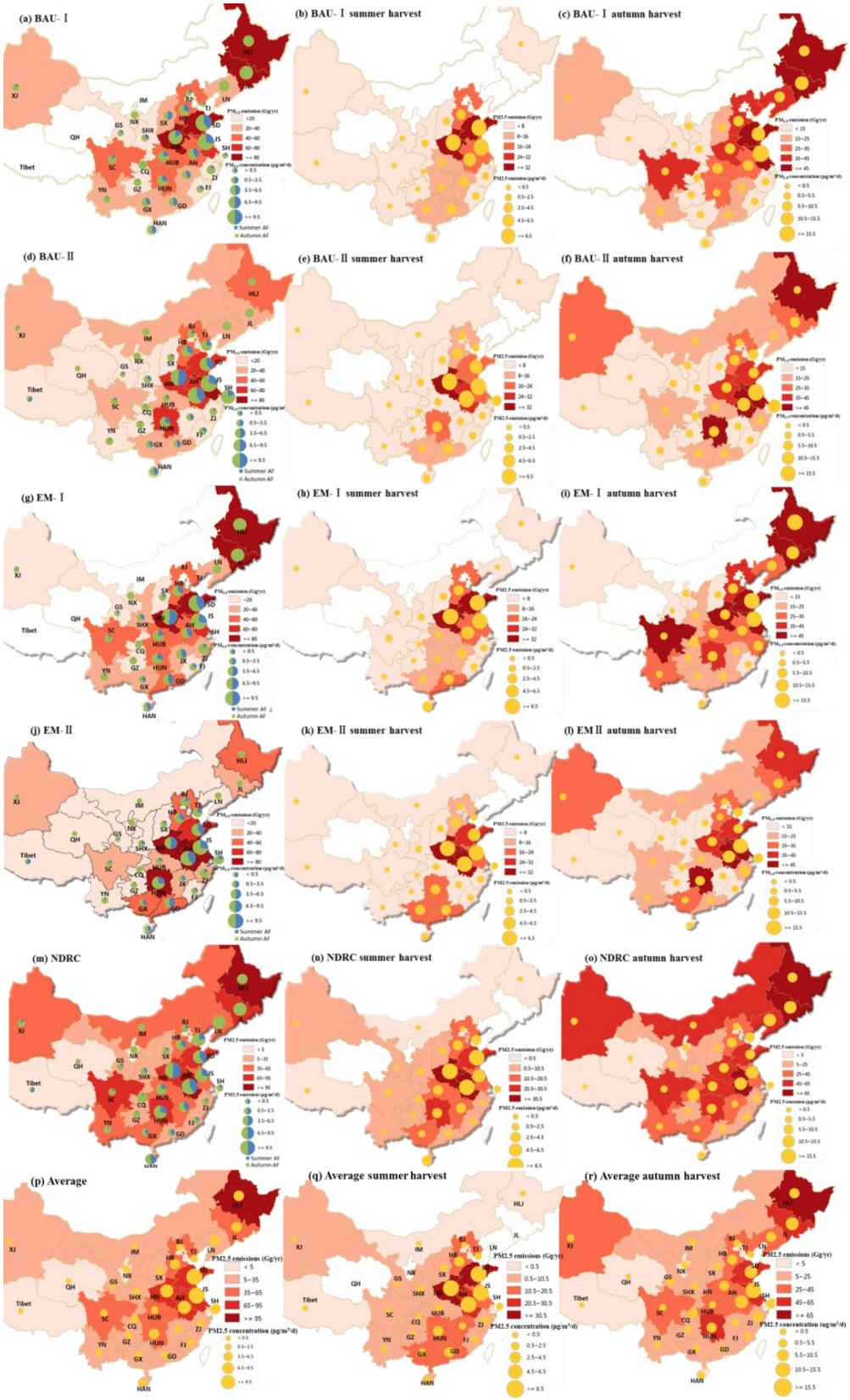

Figure 7. Spatial and temporal distribution of smoke $PM_{2.5}$ emissions and flux concentrations from agricultural field burning over China, 2012.

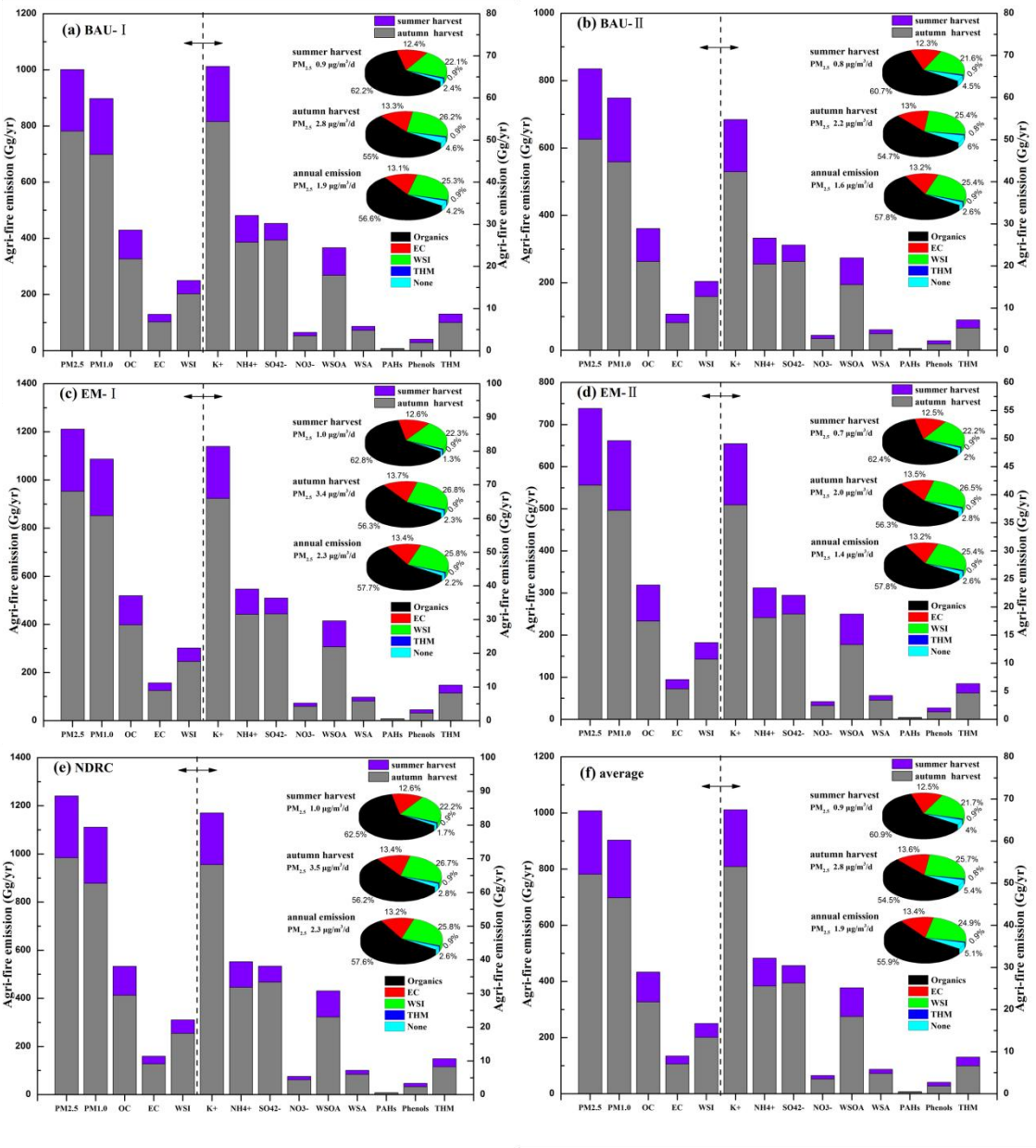

Figure 8. Nationwide $PM_{2.5}$ emissions and flux concentrations based on different burning versions. The inset pie-graphs are chemical compositions of integrated $PM_{2.5}$ from five major agricultural residue burning.